Published

ARTICLE

Aryl hydrocarbon receptor in combination with Stat1 regulates LPS-induced inflammatory responses

Akihiro Kimura,[1] Tetsuji Naka,[2] Taisuke Nakahama,[1] Ichino Chinen,[1] Kazuya Masuda,[1] Keiko Nohara,[3] Yoshiaki Fujii-Kuriyama,[4] and Tadamitsu Kishimoto[1]

[1]Laboratory of Immune Regulation, Osaka University Graduate School of Frontier Biosciences, Suita, Osaka 565-0871, Japan
[2]Laboratory for Immune Signal, National Institute of Biomedical Innovation, Ibaraki City, Osaka 567-0085, Japan
[3]Environmental Health Sciences Division, National Institute for Environmental Studies, Tsukuba, Ibaraki 305-8506, Japan
[4]Center for Tsukuba Advanced Research Alliance and Institute of Basic Medical Sciences, University of Tsukuba, 1-1-1, Tennoudai, Tsukuba 305-8577, Japan

Toll-like receptor (TLR) signals perform a crucial role in innate immune responses to pathogens. In this study, we found that the aryl hydrocarbon receptor (Ahr) negatively regulates inflammatory responses mediated by lipopolysaccharide (LPS) in macrophages. Ahr was induced in macrophages stimulated by LPS, but not by transforming growth factor (TGF)-β plus interleukin (IL)-6, which can induce Ahr in naive T cells. The production of IL-6 and tumor necrosis factor (TNF)-α by LPS was significantly elevated in Ahr-deficient macrophages compared with that in wild-type (WT) cells. Ahr-deficient mice were more highly sensitive to LPS-induced lethal shock than WT mice. Signal transducer and activator of transcription 1 (Stat1) deficiency, as well as Ahr deficiency, augmented LPS-induced IL-6 production. We found that Ahr forms a complex with Stat1 and nuclear factor-kappa B (NF-κB) in macrophages stimulated by LPS, which leads to inhibition of the promoter activity of IL-6. Ahr thus plays an essential role in the negative regulation of the LPS signaling pathway through interaction with Stat1.

CORRESPONDENCE
Tadamitsu Kishimoto:
kishimot@
imed3.med.osaka-u.ac.jp

Abbreviations used: Ahr, aryl hydrocarbon receptor; ChIP, chromatin immunoprecipitation; IMDM, Iscove's modified Dulbecco's medium; MyD88, myeloid differentiation factor 88; ODN, oligodeoxynucleotide; Stat1, signal transducer and activator of transcription 1; SOCS, suppressor of cytokine signaling 1; TLR, Toll-like receptor.

APCs such as macrophages are important for innate immune defense and for the generation and regulation of adaptive immunity against various pathogens. Activated macrophages produce proinflammatory cytokines, including IL-6, IL-12, and TNF-α, which activate T cells and induce their differentiation. It has been demonstrated that IL-6 combined with TGF-β participates in the differentiation of naive T cells into IL-17–producing T helper (Th17) cells (Bettelli et al., 2006). More recently, our group and others demonstrated that Aryl hydrocarbon receptor (Ahr), also known as dioxin receptor, is induced by TGF-β plus IL-6 in naive T cells and participates in the differentiation of Th17 cells (Kimura et al., 2008; Quintana et al., 2008; Veldhoen et al., 2008). We proved that Ahr participates in Th17 cell development through regulating activation of signal-transducer-and-activator-of-transcription 1 (Stat1), which suppresses Th17 cell differentiation (Stumhofer et al. 2006; Kimura et al., 2008).

Ahr is a ligand-activated transcription factor that belongs to the basic-helix-loop-helix-PER-ARNT-SIM family (Burbach et al., 1992; Ema et al., 1992; Fujii-Kuriyama et al., 1994). Upon binding with a ligand, Ahr undergoes a conformation change, translocates to the nucleus, and dimerizes with the Ahr nuclear translocator (Arnt). Within the nucleus, the Ahr/Arnt heterodimer binds to a specific sequence, designated a xenobiotic responsive element, which causes a variety of toxicological effects (Dragan and Schrenk, 2000; Ohtake et al., 2003; Puga et al., 2005). In immune

The Rockefeller University Press $30.00
J. Exp. Med. Vol. 206 No. 9 2027-2035
www.jem.org/cgi/doi/10.1084/jem.20090560

Supplemental Material can be found at:
http://jem.rupress.org/cgi/content/full/jem.20090560/DC1

responses, Ahr activated by ligands such as 2,3,7,8-tetrachlorodibenzo-*p*-dioxin regulates the generation of regulatory T cells and modulates Th1/Th2 balance (Funatake et al., 2005; Negishi et al., 2005). Although it has been established that Ahr performs an important role in immune regulation as well as in toxic responses, it remains unclear how Ahr modulates immune responses in individual immune cell populations. Ahr-deficient (KO) mice all die within 5 wk of birth under conventional conditions where environmental pathogens are common, in contrast to their survival in a specific pathogen–free state, which led us to hypothesize that Ahr also may play an essential role in innate immune signaling in macrophages.

The Toll-like receptor (TLR) family is a diverse group of transmembrane receptors that recognize microbial components. TLRs are expressed mainly on APCs such as macrophages and DCs and recognition of microbial products by TLRs leads to generation of a variety of signal transduction pathways that elicit rapid inflammatory reactions (Akira and Takeda, 2004). LPS is the principal active agent in the pathogenesis of endotoxin shock, which is triggered by the interaction of LPS with TLR4 and leads to the production of cytokines and other inflammatory mediators, including IL-1, IL-6, TNF-α, IL-12 and IFNs (Beutler and Rietschel, 2003). TLR4 signaling can occur via two independent pathways. One depends on myeloid differentiation factor 88 (MyD88), which results in the activation of NF-κB. This MyD88-dependent pathway is critical for the production of IL-6 and TNF-α. The other pathway is a TIR domain–containing adaptor that induces an IFN-β (TRIF)–dependent pathway, which in turn induces IFN-β via IFN regulatory factor-3 (Fitzgerald et al., 2003). A splice variant of MyD88 (MyD88s) inhibits TLR pathways by its failure to recruit IRAK4, while TGF-β also inhibits the MyD88-dependent pathway for LPS–TLR4 signaling (Burns et al., 2003; Naiki et al., 2005). We also reported that suppressor of cytokine signaling 1 (SOCS-1) negatively regulates the LPS signal pathway (Nakagawa et al., 2002; Kimura et al., 2005). Thus, while it has been demonstrated that various regulatory systems are involved in TLR signaling, the mechanisms underlying the negative regulation in TLRs signaling have not been fully elucidated.

This study deals with a novel regulatory system for TLR signaling in which Ahr negatively regulates the inflammatory responses by LPS. We demonstrate that LPS-induced proinflammatory cytokines are augmented in Ahr-deficient macrophages compared with those in WT cells, and that Ahr-deficient mice are more susceptible to endotoxin shock induced by LPS. We also provide evidence that Ahr interacts with Stat1 and NF-κB and that the Ahr–Stat1 complex controls NF-κB-dependent proinflammatory responses by LPS.

RESULTS

Increased LPS-induced production of proinflammatory cytokines in Ahr deficient macrophages

Our group and others previously reported that Ahr is induced in naive T cells stimulated by TGF-β plus IL-6, which participates in the induction of Th17 cell differentiation (Kimura et al., 2008; Quintana et al., 2008; Veldhoen et al., 2008). In this study, we used Western blot analysis to investigate Ahr expression in peritoneal macrophages stimulated by LPS, CpG-oligodeoxynucleotides (ODNs), and TGF-β plus IL-6. Ahr was expressed in peritoneal macrophages stimulated by LPS and CpG-ODN, but not by TGF-β plus IL-6 (Fig. 1 A), indicating that Ahr is induced by TLR signaling in those cells and that its expression pattern in macrophages and T cells is different. We next used Ahr KO peritoneal macrophages to examine whether Ahr affects LPS-induced proinflammatory cytokine production. As shown in Fig. 1 B, the levels of IL-6, TNF-α, and IL-12p40 were significantly elevated by LPS in Ahr KO peritoneal macrophages compared with those in WT cells. Next, we used a retroviral system to investigate whether Ahr reconstitution could reverse the phenotype in Ahr KO peritoneal macrophages and found that infection with Ahr in Ahr-deficient cells restored the overproduction of IL-6 (Fig. S1 A). We also examined TLR4 expression in WT and Ahr KO peritoneal macrophages, which showed the same pattern (unpublished data), indicating that the LPS signal is normally transmitted from the plasma membrane to the cytoplasm between WT and Ahr KO cells. To examine the effect of Ahr on LPS signaling, we established a mouse macrophage-like cell line (RAW cells) that constitutively expressed Ahr (RAW/Ahr). With RAW/Neo cells functioning as control, RAW/Ahr cells were treated with LPS, and LPS-induced production of proinflammatory cytokines was examined by means of ELISA. It was found that IL-6 and IL-12p40 production by LPS was inhibited in Ahr-overexpressing RAW cells compared with that in RAW/Neo cells (Fig. 1 C).

It has been recently reported that Ahr agonists in culture medium are important for Th17 cell differentiation, in which Iscove's modified Dulbecco's medium (IMDM), a medium that is richer in amino acids that can give rise to Ahr agonists, enhances Th17 cell development more than RPMI medium (Veldhoen et al., 2009). We therefore tested whether IMDM affects increased LPS-induced production of proinflammatory cytokines in WT- and Ahr-deficient macrophages. Although IMDM suppressed LPS-induced IL-6 production in WT peritoneal macrophages when compared with RPMI medium, its production was inhibited at the same rate as in Ahr KO cells (Fig. S1 B). These results indicate that natural ligands for Ahr in this culture medium do not affect the regulation of LPS signaling by Ahr.

Because it is known that macrophages produce an anti-inflammatory cytokine, IL-10, to control the overproduction of inflammatory cytokines (Moore et al., 2001), we compared LPS-induced IL-10 production in WT and Ahr KO peritoneal macrophages. In contrast to proinflammatory cytokine production, LPS-induced IL-10 production was inhibited in Ahr KO peritoneal macrophages compared with that in WT cells (Fig. 1 D). These results demonstrate that Ahr has an antiinflammatory function in macrophages under the LPS–TLR4 signaling pathway. Because hypoproduction

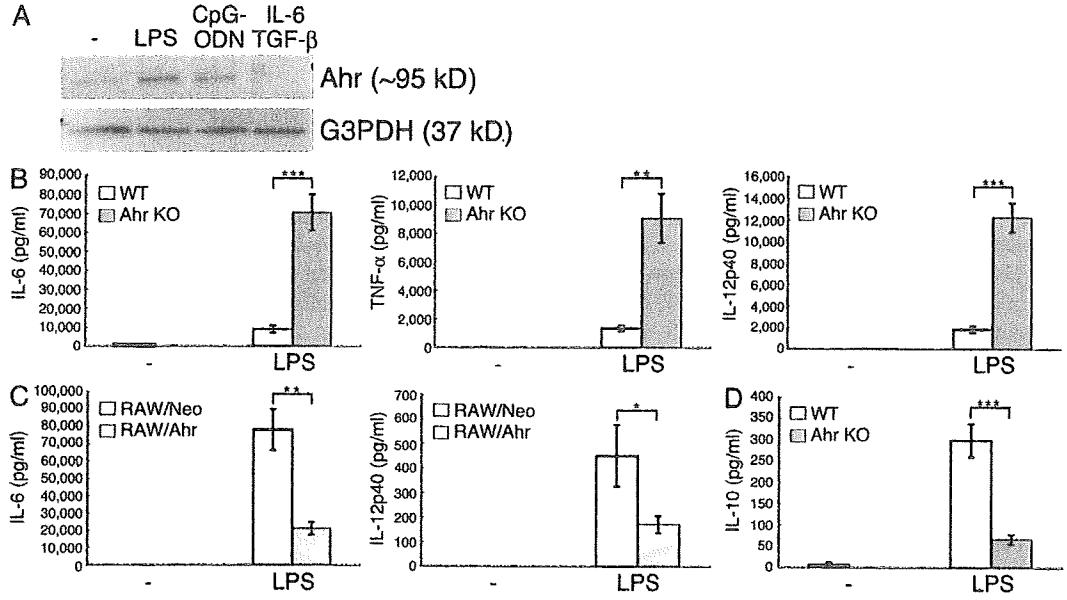

Figure 1. Ahr deficiency augments LPS-induced proinflammatory responses in macrophages. (A) Peritoneal macrophages were stimulated with LPS, CpG-ODN, and TGF-β plus IL-6 for 24 h. The cells were lysed and subjected to immunoblotting (IB) analysis for the expression of Ahr and G3PDH. Data are from one representative of three independent experiments. (B–D) WT and Ahr KO peritoneal macrophages or RAW/Neo and RAW/Ahr cells were stimulated with LPS. Supernatants were collected 24 h after stimulation, and the production of IL-6, TNF-α, IL-12p40, and IL-10 were measured by means of ELISA. Data show means ± SEM of three independent experiments (*, $P < 0.05$; **, $P < 0.005$; ***, $P < 0.001$).

of IL-10 may cause hyperproduction of proinflammatory cytokines in Ahr KO peritoneal macrophages under LPS stimulation, we tested whether the addition of IL-10 to Ahr KO cells stimulated by LPS normalizes the overproduction of proinflammatory cytokine. Although IL-10 inhibited LPS-induced IL-6 production in Ahr KO cells by ~40% compared with that by LPS stimulation only, its production was higher than that in WT cells stimulated by LPS (Fig. S2). Additionally, we found that RAW cells were not able to produce IL-10 under LPS stimulation (unpublished data), which suggests that the inhibition of LPS-induced proinflammatory cytokines in RAW/Ahr cells is unrelated to IL-10. These results indicate that Ahr regulates the production of LPS-induced proinflammatory cytokines independently of IL-10.

Ahr-deficient mice are hyperresponsive to LPS

Because Ahr KO peritoneal macrophages showed a higher level of LPS-induced proinflammatory cytokine production than WT cells, we asked whether Ahr KO mice were more susceptible to LPS-induced toxicity. 6-wk-old WT and Ahr KO mice were injected intraperitoneally with 7.5 mg/kg of LPS. As shown in Fig. 2 A, all Ahr KO mice died within 60 h of being injected, but their WT littermates did not. We next measured serum levels of IL-6 and TNF-α in WT and Ahr KO mice after the LPS challenge. The serum IL-6 level in WT mice peaked 2 h after LPS administration, and then returned to the baseline level by 24 h, which is consistent with previously reported findings (Basu et al., 1997). In contrast, although serum IL-6 levels in Ahr KO mice increased similarly to those in WT mice until 2 h after LPS challenge, serum IL-6 in Ahr KO mice maintained the same level for 2–12 h and then increased again (Fig. 2 B). On the other hand, serum TNF-α levels in Ahr KO mice were significantly higher than in WT mice 2 h after LPS administration, but the kinetics were similar in the two groups of mice (Fig. 2 C). These results demonstrate that Ahr is involved in the negative regulation of LPS responses in vivo as well.

Stat1 interacts with Ahr and regulates LPS-induced inflammatory responses in macrophages

We previously reported that Ahr interacts with Stat1 and inhibits its activation in the process of Th17 cell differentiation (Kimura et al., 2008). To examine whether Ahr can bind with Stat1 in macrophages as it does in T cells, peritoneal macrophages were stimulated with LP, followed by verification (via immunoprecipitation and Western blotting) of the interaction between Ahr and Stat1. The results demonstrated that Ahr interacted with Stat1 in macrophages after activation with LPS (Fig. 3 A). To verify the involvement of Stat1 in LPS-stimulated cytokine production, WT and Stat1 KO peritoneal macrophages were stimulated with LPS, and the protein levels of IL-6 and IL-10 were measured by means of ELISA. Similar to that in Ahr KO peritoneal macrophages, LPS-induced IL-6 production was significantly augmented in Stat1 KO cells, whereas IL-10 production was inhibited compared with that in WT cells (Fig. 3 B). We confirmed that Ahr was normally induced by LPS in the absence of Stat1 (Fig. S3 A), indicating that hyperproduction of IL-6 in Stat1

KO peritoneal macrophages stimulated by LPS is not caused by the absence of Ahr.

We previously demonstrated that Ahr inhibits Stat1 activation in naive T cells under Th17-polarizing conditions (TGF-β plus IL-6; Kimura et al., 2008). In macrophages, however, Ahr prolonged Stat1 activation by LPS. LPS-induced Stat1 activation was diminished in Ahr KO macrophages compared with that in WT cells (Fig. 3 C). On the other hand, LPS-induced Stat1 activation was prolonged in RAW/Ahr cells compared with that in RAW/Neo cells (Fig. 3 C). Because it has been reported that LPS-dependent Stat1 phosphorylation is mainly dependent on IFN-β (Toshchakov et al., 2002) and that SOCS proteins are important for regulating Stat1 activation (Yoshimura et al., 2007), we examined both LPS-induced IFN-β production and the expression of SOCS-1 and SOCS-3 in WT and Ahr KO peritoneal macrophages stimulated with LPS. We found no changes in IFN-β production or SOCSs expression in WT and Ahr KO cells after LPS stimulation (Fig. S3, B and C), indicating that the suppression of Stat1 activation by LPS in Ahr KO macrophages occurs independently of IFN-β and SOCSs. Collectively, these findings suggest that Ahr may directly protect the inactivation of Stat1 in macrophages through interacting with it, followed by regulation of LPS signaling.

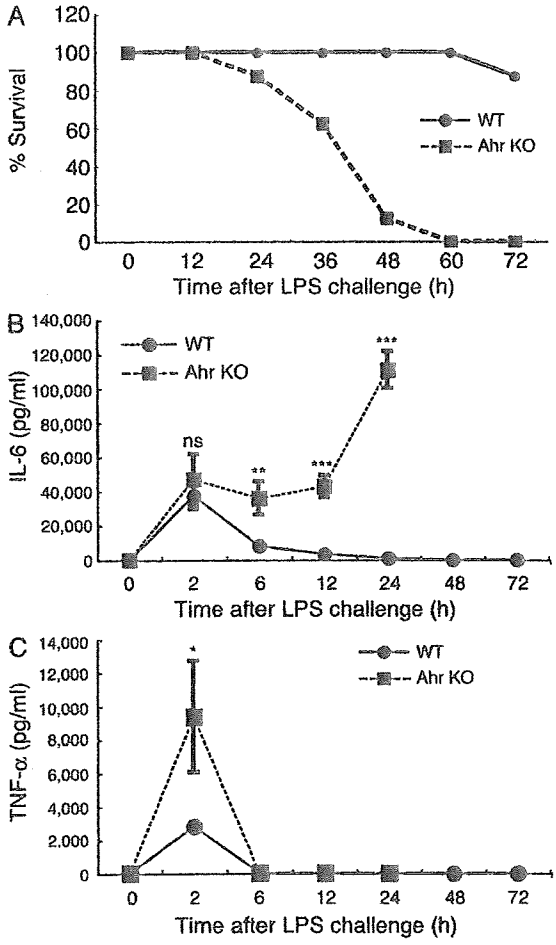

Figure 2. Hypersensitivity of Ahr KO mice to LPS in vivo. 6-wk-old Ahr KO mice and littermate WT mice ($n = 10$ for each) were i.p. injected with 7.5 mg/kg of LPS. (A) Lethality was observed over 60 h after LPS challenge. Data are representative of two independent experiments. (B and C) Serum levels of IL-6 and TNF-α between WT and Ahr KO mice were measured by ELISA at indicated time points after LPS challenge. Data show means ± SEM of three independent experiments (*, $P < 0.05$; **, $P < 0.01$; ***, $P < 0.001$).

Ahr–Stat1 complex binds to NF-κB and suppresses its transcriptional activity, but not its DNA-binding capacity

The production of proinflammatory cytokines such as IL-6 and TNF-α by LPS is induced via the MyD88-dependent NF-κB pathway (Kawai et al., 1999; Beutler and Rietschel, 2003). It has also been reported that Ahr combines with NF-κB, and that this complex regulates several signal pathways (Tian et al., 1999, 2002; Vogel et al., 2007). We speculated that the Ahr–Stat1 complex might interact with NF-κB, followed by regulation of the NF-κB pathway by the resultant complex. To test this hypothesis, we first examined whether

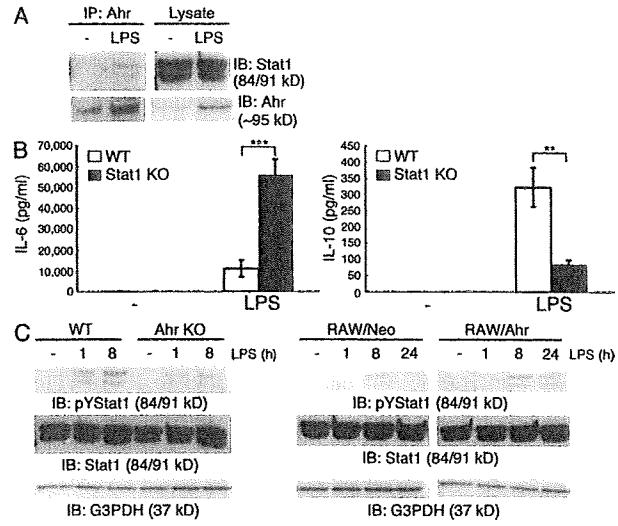

Figure 3. Association between Ahr and Stat1 in macrophages. (A) Peritoneal macrophages were isolated from BALB/c mice and stimulated by LPS for 24 h. Interaction between Ahr and Stat1 was examined by means of immunoprecipitation (IP) and Western blotting. Data are from one representative of three independent experiments. IB, immunoblot. (B) WT and Stat1 KO peritoneal macrophages were stimulated with LPS. Supernatants were collected 24 h after stimulation, and the production of IL-6 and IL-10 were measured by means of ELISA. Data show means ± SEM of three independent experiments (**, $P < 0.005$; ***, $P < 0.001$). (C) WT and Ahr KO peritoneal macrophages or RAW/Neo and RAW/Ahr cells were incubated with LPS at the indicated time points. Whole-cell lysates were used for immunoblotting analysis with anti-phosphotyrosine Stat1, Stat1, and G3PDH antibodies (Ab). Data are from one representative of three independent experiments.

Ahr interacts with NF-κB together with Stat1. COS7 cells were transiently transfected with Ahr, NF-κB p50, and Stat1 and subjected to coimmunoprecipitation analysis. As shown in Fig. 4 A, Ahr interacted with NF-κB p50 (lane 6) and formed a complex together with NF-κB p50 and Stat1 (lane 5). Furthermore, to determine whether endogenous Ahr forms a complex together with endogenous Stat1 and NF-κB p50, peritoneal macrophages were stimulated with LPS, followed by verification by means of immunoprecipitation and Western blotting of the association of their endogenous proteins. We also found that Ahr interacts with Stat1 and NF-κB p50 endogenously in peritoneal macrophages activated by LPS (Fig. 4 B).

We next examined the effect of Ahr on LPS-induced activation of the IL-6 promoter. RAW cells were transiently transfected with a reporter plasmid containing the promoter of IL-6 combined with either Ahr or a control vector. After treatment with LPS, luciferase activities were measured with the dual luciferase reporter assay system. LPS-induced activation of the IL-6 promoter was significantly suppressed in RAW cells overexpressing Ahr (Fig. 4 C), which suggests that Ahr inhibits the NF-κB transcriptional activity on LPS-induced IL-6 production. For further investigation of how Ahr regulates LPS-induced NF-κB activation, we used the TransAM assay to assess NF-κB DNA binding activity between RAW/Neo and RAW/Ahr cells stimulated by LPS. Ahr showed no significant influence on LPS-induced NF-κB DNA binding activity between those cells (Fig. 4 D). Similarly, NF-κB bound to its target DNA upon LPS stimulation of both WT- and Ahr-KO peritoneal macrophages (Fig. 4 D).

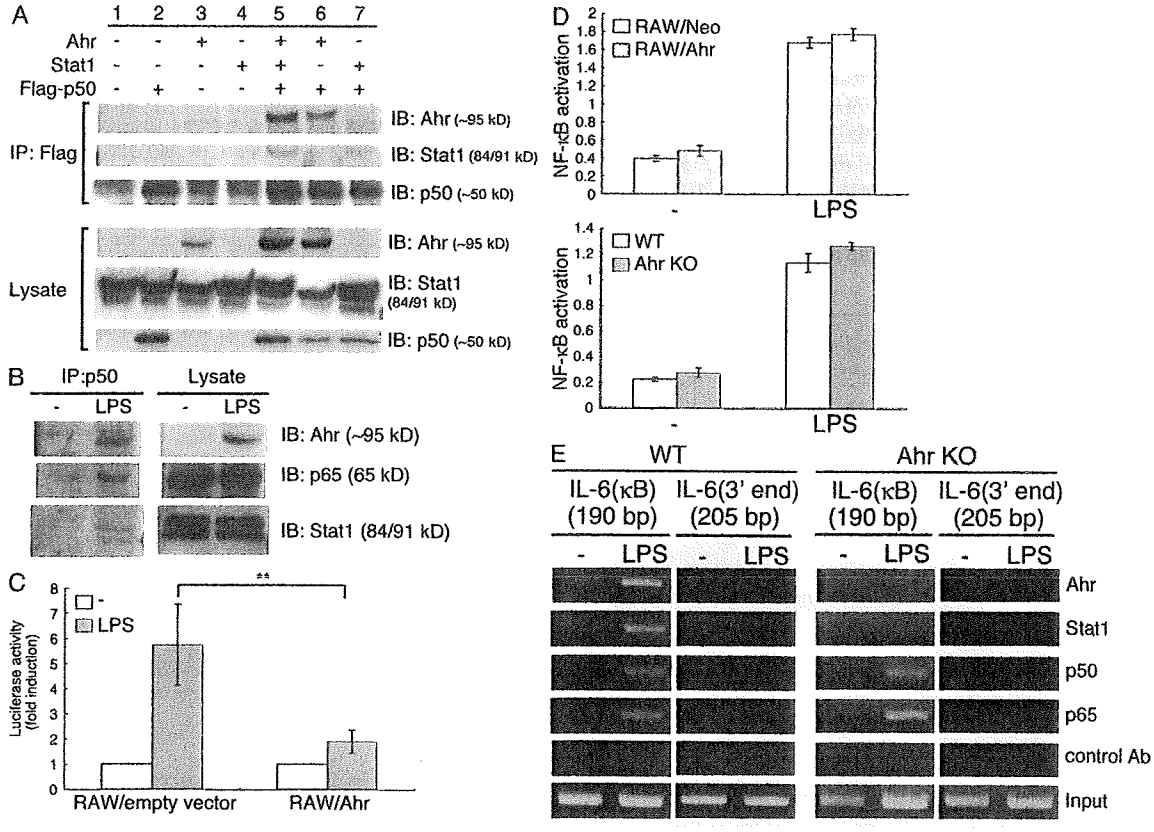

Figure 4. Ahr inhibits LPS-induced NF-κB transcriptional activity together with Stat1. (A) COS7 cells were cotransfected with Ahr, Stat1, and p50-Flag. After 24 h, the cells were lysed and immunoprecipitated with anti-Flag Ab, followed by detection of Ahr, Stat1, and p50 by means of Western blotting. Data are from one representative of three independent experiments. IP, immunoprecipitation; IB, immunoblot. (B) Peritoneal macrophages were stimulated with LPS for 24 h. Whole-cell lysates were immunoprecipitated with anti-p50 antibody, after which Ahr, p65, and Stat1 were detected with Western blotting. Data are from one representative of three independent experiments. (C) RAW cells were transiently cotransfected with luciferase reporter gene construct of the murine IL-6 promoter and an expression vector for Ahr (RAW/Ahr) or empty control expression vector (RAW/empty vector). 6 h after transfection, cells were stimulated with LPS for 12 h. Luciferase assay and quantitation were performed as described in Materials and methods. Data show means ± SEM of three independent experiments (**, $P < 0.02$). (D) RAW/Neo and RAW/Ahr or WT and Ahr KO peritoneal macrophages were stimulated with LPS for 24 h NF-κB binding activity was examined using TransAM assay. Data show means ± SEM of three independent experiments. (E) Peritoneal macrophages from WT and Ahr KO mice were stimulated with LPS for 4 h, and the ChIP assay was performed using anti-p50, anti-p65, anti-Stat1, and anti-Ahr antibodies. Purified DNA fragments were amplified using primers specific for the IL-6 promoter. Data are from one representative of three independent experiments.

Cytosolic IκB-α is reportedly degraded upon activation of NF-κB (Brown et al., 1993), and we also found no difference in IκB-α degradation in macrophages stimulated by LPS with or without Ahr (Fig. S4). These findings demonstrate that Ahr suppresses the NF-κB transcriptional activity of the IL-6 promoter, but not its DNA-binding capacity. It has further been reported that IL-6 production is required to induce IκBζ via the Myd88-dependent NF-κB pathway in LPS signaling, followed by the association of IκBζ with p50 and recruitment of the resultant complex to the IL-6 promoter (Yamamoto et al., 2004). We therefore examined whether Ahr affects IκBζ induction by LPS and found no difference in its induction by LPS in RAW/Ahr and RAW/Neo cells (Fig. S5). This result is consistent with that illustrated in Fig. 4 D, which shows that Ahr does not affect the NF-κB DNA-binding activity. These findings indicate that Ahr selectively inhibits NF-κB transcriptional activity in the LPS signaling pathway.

We further examined whether upon LPS stimulation the Ahr–Stat1 complex can interact with NF-κB on the promoter region of proinflammatory cytokines and then suppress LPS-induced NF-κB transcriptional activation and inflammatory cytokine production. We performed the chromatin immunoprecipitation (ChIP) assay to determine whether Ahr and Stat1 are recruited to the IL-6 promoter in response to LPS in combination with NF-κB. Peritoneal macrophages from WT and Ahr KO mice were stimulated with LPS for 4 h, and the ChIP assay was performed using antibodies for detection of Ahr, Stat1, p50, and p65, and it was found that although p50 and p65 were recruited to the IL-6 promoter in response to LPS in both cells, Ahr and Stat1 bound to the IL-6 promoter region in WT, but not in Ahr KO cells (Fig. 4 E). These results indicate that Ahr, in combination with Stat1, regulates LPS-induced proinflammatory cytokine production in macrophages through inhibition of NF-κB transcriptional activity in their promoter region.

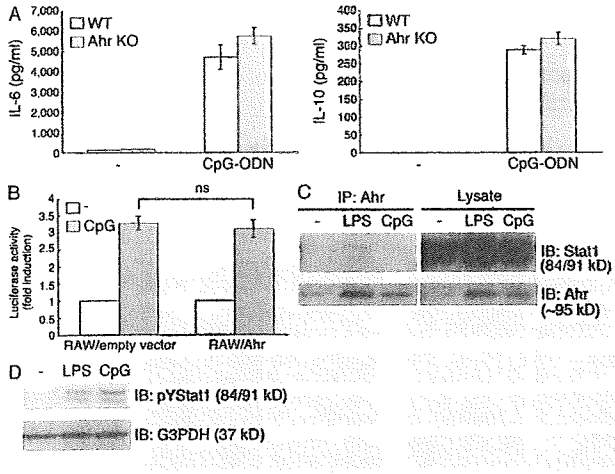

Figure 5. Ahr has no influence in CpG-ODN signaling pathway. (A) WT and Ahr KO peritoneal macrophages were stimulated with CpG-ODN for 24 h. The production of IL-6 and IL-10 were measured by means of ELISA. Data show means ± SE of three independent experiments. (B) RAW cells were transiently cotransfected with luciferase reporter gene construct of the murine IL-6 promoter and an expression vector for Ahr (RAW/Ahr) or empty control expression vector (RAW/empty vector). 6 h after transfection, cells were stimulated with CpG-ODN for 12 h. Luciferase assay and quantitation were performed as described in Materials and methods. Data show means ± SEM of three independent experiments. Peritoneal macrophages were stimulated with LPS and CpG-ODN. (C) Cells were lysed, immunoprecipitated by Ahr, and analyzed by Western blotting with anti-Stat1 Ab. IP, immunoprecipitation; IB, immunoblot. (D) Whole-cell lysates subjected to Western analysis with anti-pYStat1 antibodies. Data are from one representative of three independent experiments.

Ahr does not participate in CpG-ODN signaling

As shown in Fig. 1 A, Ahr was induced in peritoneal macrophages stimulated by CpG-ODN and LPS. We therefore asked whether Ahr regulates the CpG-ODN–TLR9 pathway. WT and Ahr KO peritoneal macrophages were stimulated with CpG-ODN, and the protein levels of IL-6 and IL-10 were measured by means of ELISA. Surprisingly, we found that Ahr deficiency had no effect on their production by CpG-DNA (Fig. 5 A) and that CpG-ODN–induced activation of the IL-6 promoter was similar in RAW cells with or without Ahr (Fig. 5 B). Thus, Ahr is not capable of regulating the CpG-ODN signaling pathway despite its expression in peritoneal macrophages stimulated with CpG-ODN.

To understand why Ahr has no effect on CpG-ODN-induced pro- and antiinflammatory cytokine production, we assessed the interaction between Ahr and Stat1 in LPS- or CpG-ODN–treated peritoneal macrophages. As shown in Fig. 3 A, although Ahr interacted with Stat1 under LPS stimulation, hardly any binding of Ahr with Stat1 could be detected in CpG-ODN–treated cells (Fig. 5 C). However, CpG-ODN activated Stat1 to the same degree as did LPS stimulation (Fig. 5 D), indicating that the complex formation of Ahr with Stat1 is independent of Stat1 activation. These results suggest that it may be required for some natural ligand for Ahr to form the complex with Stat1 and that LPS may be able to induce some natural ligand for Ahr, but not CpG-ODN.

DISCUSSION

Ahr is a ligand-inducible transcription factor, which has been shown to regulate the expression of a variety of genes, including those encoding for cytochrome P450 enzymes. In addition, Ahr activation by ligands such as dioxin has been linked to alterations in cell proliferation, apoptosis, tumor promotion, development, and reproductive functions (Puga et al., 2000; Shimizu et al., 2000; Bonnesen et al., 2001). A growing number of studies have recently detailed the various effects of Ahr on the immune system, especially the development of Th17 cells (Kimura et al., 2008; Quintana et al., 2008; Veldhoen et al., 2008). Because we found that Ahr-KO mice all die under conventional conditions, it was expected that Ahr might also participate in the innate immune system, which is capable of recognizing a wide variety of

pathogens and rapidly inducing various antimicrobial and inflammatory responses. In this study, we identified an important role of Ahr in TLR signaling, that is, Ahr combined with Stat1 controls LPS–TLR4–mediated pro- and antiinflammatory cytokine production.

Initially, we demonstrated that TLR ligands such as LPS, but not IL-6 in combination with TGF-β, induced Ahr expression in macrophages and that, whereas the production of proinflammatory cytokines such as IL-6, TNF-α, and IL-12p40 was drastically increased upon LPS stimulation, production of the antiinflammatory cytokine IL-10 was inhibited in the absence of Ahr. In addition, we found that Ahr-deficient mice were highly susceptible to LPS-induced toxicity. The levels of serum IL-6 and TNF-α in Ahr KO mice were higher than those in WT mice after LPS challenge. These findings indicate that Ahr contributes to the negative regulation of the LPS signal pathway both in vivo and in vitro.

We also found that Ahr forms a complex with Stat1 and NF-κB, which is consistent with previous findings that Ahr interacts with several transcriptional factors, such as Stat1 and NF-κB (Tian et al., 1999, 2002; Vogel et al., 2007; Kimura et al., 2008). An important finding of our current study is that Stat1 deficiency, like Ahr deficiency, led to an increase in LPS-induced IL-6 production, but suppressed production of the LPS-induced antiinflammatory cytokine IL-10. However, it was previously reported that Stat1-deficient mice are resistant to LPS-induced shock (Karaghiosoff et al., 2003), which seems to conflict with our finding that Stat1-deficient macrophages produce more IL-6 and less IL-10 compared with those produced in WT cells. Stat1 contributes to the development of endotoxin shock through its central role in IFN responses, which are secondarily induced by LPS (Karaghiosoff et al., 2003). Stat1 deficiency therefore shows resistance to LPS-induced shock in vivo through blocking LPS-induced secondary cytokine (IFN) signaling. We speculate that Stat1 takes part in not only LPS-induced secondary responses (IFN responses) in vivo but also in direct signaling of LPS in vitro through interacting with NF-κB and Ahr; in the latter function Stat1 has the property to suppress LPS-NF-κB signaling.

The findings that Ahr inhibits LPS-induced activation of the IL-6 promoter and interacts in combination with both NF-κB and Stat1 on the same region of the IL-6 promoter suggest that the Ahr–Stat1 complex may control LPS-induced proinflammatory responses by inhibiting NF-κB transcriptional activity. In fact, NF-κB DNA-binding activity was not inhibited by Ahr, which is consistent with the finding that Ahr did not affect the expression of IκBζ via the LPS-MyD88-dependent pathway. At present, however, the detailed mechanism of Ahr in suppressing NF-κB transcriptional activity remains poorly understood. Nuclear receptors in combination with coactivators and corepressors can switch the transcriptional activity of several transcriptional factors on and off, respectively. It was recently reported that Ahr repressor (Ahrr), known as an Ahr negative regulator, represses estrogen receptor α–mediated transcriptional activation through interacting directly with ERα on the promoter sequences of estrogen receptor–target genes (Kanno et al., 2008). This seems to imply that the Ahr–Stat1 complex may inhibit LPS-induced NF-κB transcriptional activity via a corepressor such as Ahrr.

Two groups in addition to ours recently reported that Ahr participates in Th17 cell differentiation (Kimura et al., 2008; Quintana et al., 2008; Veldhoen et al., 2008). In our study, we provided evidence that Ahr is involved in the differentiation of Th17 cells by inhibiting Stat1 activation, which suppresses Th17 cell differentiation, under Th17-polarizing conditions (TGF-β plus IL-6). Stat1 activation was eliminated 24 h after stimulation with TGF-β plus IL-6 in WT naive T cells, whereas its activation was maintained in Ahr-deficient naive T cells (Kimura et al., 2008). In contrast, Stat1 activation by LPS was inhibited in Ahr-deficient macrophages, compared with that in normal macrophages. These findings indicate that Stat1 activation is differentially regulated by Ahr in T cells and macrophages. Ahr is known to perform a dual function in controlling intracellular protein levels, serving both as a transcriptional factor and as a ligand-dependent E3 ubiquitin ligase (Ohtake et al., 2007). It is also possible that, although Ahr regulates the activation of Stat1 through the degradation of activated Stat1 by functioning as a ligand-dependent E3 ubiquitin ligase in the generation of Th17 cells, it acts like a transcriptional factor and cooperates with Stat1 to regulate NF-κB transcriptional activation in LPS-activated macrophages. Thus, the Ahr–Stat1 combination controls immune responses in different ways depending on the immune cell population.

The CpG-ODN–TLR9 signaling pathway and the LPS–TLR4 signaling pathway induce proinflammatory cytokines such as IL-6 via MyD88-NF-κB (Akira and Takeda, 2004). However, our findings demonstrate that Ahr is incapable of regulating the production of pro- and antiinflammatory cytokines by CpG-ODN, although it is induced in peritoneal macrophages stimulated with CpG-ODN. Interestingly, Ahr interacted with Stat1 in the peritoneal macrophages under stimulation with LPS, but not with CpG-ODN, even though the level of Stat1 activation was the same for these two stimulations, which may account for the difference between the LPS and CpG-ODN signaling pathways in the regulation by Ahr of pro- and antiinflammatory cytokine production. Given that Ahr forms the complex together with Stat1 and p50 on the IL-6 promoter region and regulates NF-κB transcriptional activity, Stat1 may be required for the inhibition of NF-κB transcriptional activity by Ahr. Some natural ligand may be required when Ahr forms the complex with Stat1, followed by the regulation of NF-κB.

Our preliminary data show that IL-6 suppresses LPS-induced Ahr expression in macrophages (unpublished data). As seen in Fig. 1 A, the expression of Ahr in macrophages was inhibited by IL-6 in combination with TGF-β. In this study, we demonstrated that Ahr performs an antiinflammatory function in macrophages. It can thus be speculated that IL-6 may amplify proinflammatory responses in macrophages

through inhibiting the expression of Ahr, which suppresses LPS-induced proinflammatory responses. In T cells, on the other hand, IL-6 combined with TGF-β induces the expression of Ahr, which participates in Th17 cell differentiation. IL-6 thus promotes proinflammatory responses through the differential regulation of Ahr expression in macrophages and T cells.

To summarize, we have identified and characterized a novel regulatory mechanism of the TLR signaling pathway in which Ahr in combination with Stat1 concurrently controls LPS-induced pro- and antiinflammatory cytokine production. We have also provided evidence that Ahr differentially regulates Stat1 activation and NF-κB transcriptional activity in T cells and macrophages, respectively. This suggests that Ahr may control several immune responses through the regulation of transcriptional factors, such as the Stat and NF-κB families, and be involved in several autoimmune diseases. It is necessary to gain an understanding of how Ahr regulates the immune system in various immune cells such as T cells, B cells, macrophages and dendritic cells. Further studies using each immune cell–specific Ahr conditional KO mice will define the functions of Ahr in immunity and several autoimmune diseases.

MATERIALS AND METHODS

Mice. C57BL/6 WT mice were obtained from CLEA Japan, Inc. Ahr KO mice and Stat1 KO mice (C57BL/6 background) were provided by Y. Fujii-Kuriyama (University of Tsukuba, Tsukuba, Japan) and T. Naka (National Institute of Biomedical Innovation, Osaka, Japan), respectively. All mice were maintained under specific pathogen-free conditions. All animal experiments were performed in accordance with protocols approved by the Institutional Animal Care and Use Committees of the Graduate School of Frontier Bioscience, Osaka University. WT and Ahr KO mice were injected i.p. with the indicated amounts of LPS (*Escherichia coli*; Sigma-Aldrich) for the indicated periods of time.

Cell culture and reagents. Peritoneal macrophages were prepared as previously described (Kimura et al., 2005). The thioglycolate-elicited peritoneal macrophages and a mouse macrophage cell line (RAW cells) were cultured in RPMI 1640 with 10% FCS, 100 μg/ml streptomycin, and 100 U/ml penicillin G. RAW cells were stably transfected with Ahr cDNAs (donated by Y. Fujii-Kuriyama). Stably transfected RAW mutant lines (RAW/Neo, RAW/Ahr) were maintained in the presence of 500 μg/ml G418. COS7 cells were cultured in DME with 10% FCS, 100 μg/ml streptomycin, and 100 U/ml penicillin G. We stimulated the cells with 1 μg/ml LPS (*E. coli*; Sigma-Aldrich), 1 μM phosphorothioate-modified CpG-ODN, 20 ng/ml mouse IL-6 and 2 ng/ml human TGF-β1 (both from R&D Systems) for the indicated periods of time.

Cytokine ELISA. The cells were stimulated with 1 μg/ml LPS (*E. coli*; Sigma-Aldrich) and 1 μM phosphorothioate-modified CpG-ODN for 24 h. Mouse IL-6, TNF-α, IL-12p40, and IL-10 from either the supernatants or the serum were measured by means of ELISA according to the manufacturer's instructions (R&D Systems).

Immunoprecipitation and Western blotting. Peritoneal macrophages were cultured with 1 μg/ml LPS or 1 μM phosphorothioate-modified CpG-ODN for 24 h and then lysed with a lysis buffer (1% NP-40, 20 mM Tris-HCl, ph 7.5, 150 mM NaCl, 10 mM Na_2VO_4, 0.5 mM DTT, and 1/100 protease inhibitor cocktail). Ahr and p50 were immunoprecipitated with anti-Ahr (BIOMOL International) and anti-p50 (Santa Cruz Biotechnology, Inc.), respectively, and then subjected to SDS-PAGE. Whole-cell lysates and the immunocomplex were analyzed with Western blotting using anti-Stat1 (BD), anti-p65 (Santa Cruz Biotechnology, Inc.), or anti-Ahr (BIOMOL International L.P.). COS7 cells were cotransfected with 1 μg of pEF-BOS-Ahr, pEF-BOS-Stat1, and pEF-BOS-p50-Flag with the aid of FuGENE 6 (Roche). Cells were lysed with lysis buffer and lysates were immunoprecipitated with anti-Flag M2 (Sigma-Aldrich). Immunoprecipitated samples were analyzed by means of Western blotting by using anti-Ahr (BIOMOL), anti-Stat1 (BD) and anti-p50 (Santa Cruz Biotechnology, Inc.).

Activation of Stat1. WT and Ahr KO peritoneal macrophages or RAW/Neo and RAW/Ahr cells were incubated with 1 μg/ml LPS for the time indicated, and cells were lysed with a lysis buffer. Whole-cell lysates were then analyzed by means of Western blotting using anti–phospho-Stat1 (Tyr701; Cell Signaling Technology).

Luciferase assay. RAW cells were transfected with 1 μg of the reporter plasmid and, in cotransfection experiments, with 0.1 μg of pRL-TK for use as an internal control reporter and 1 μg of pEF-BOS-Ahr or an empty vector (pEF-BOS). Cells were stimulated with 1 μg/ml LPS or 1 μM phosphorothioate-modified CpG-ODN for 12 h and lysed with luciferase lysis reagent (Promega). Luciferase activity was determined with a commercial dual-luciferase reporter assay system (Promega) according to the manufacturer's instructions. Relative light units of *Firefly* luciferase activity were normalized with *Renilla* luciferase activity.

TransAM assay. RAW/Neo and RAW/Ahr cells or WT and Ahr KO peritoneal macrophages were stimulated with 1 μg/ml LPS for 24 h. Nuclear extraction was performed with a nuclear extraction kit (Active Motif). 10 μg of nuclear extraction protein was used for assessing the NF-κB binding activity with the NF-κB (p50) TransAM Assay (Active Motif) according to the manufacturer's instructions.

ChIP assay. The ChIP assay was performed essentially according to Upstate Biotechnology's protocol. In brief, WT and Ahr KO peritoneal macrophages were stimulated with 1 μg/ml LPS for 12 h, and then fixed with formaldehyde for 10 min. The cells were lysed, sheared by sonication, and incubated overnight with specific antibodies, followed by incubation with protein A-agarose saturated with salmon sperm DNA (Vector Laboratories). Precipitated DNAs were analyzed by quantitative PCR (35 cycles) using primers 5′-CGATGCTAAACGACGTCACATTGTGCA-3′ and 5′-CTCCAGAGCAGAATGAGCTACAGACAT-3′ for the κB site in the IL-6 promoter.

Statistical analysis. Student's *t* test was used to analyze data for significant differences. Values of $P < 0.05$ were regarded as significant.

Online supplemental material. Fig. S1 shows that Ahr regulates LPS-induced production of IL-6 with or without natural ligands for Ahr in culture medium. Fig. S2 shows that that hypoproduction of IL-10 does not cause hyperproduction of proinflammatory cytokines in Ahr KO peritoneal macrophages under LPS stimulation. Fig. S3 shows the expression of Ahr in Stat1 KO peritoneal macrophages and the induction of IFN-β and SOCS family members in Ahr KO cells. Fig. S4 shows the IκB-α degradation in WT and Ahr KO macrophages stimulated by LPS. Fig. S5 shows the IκBζ expression in RAW/Neo and RAW/Ahr cells stimulated by LPS. Online supplemental material is available at http://www.jem.org/cgi/content/full/jem.20090560/DC1.

This work was supported by the Program for Promotion of Fundamental Studies in Health Sciences of the National Institute of Biomedical Innovation and Chugai-Roche Pharmaceutical Co. Ltd, Tokyo, Japan.

The authors have no conflicting financial interests.

Submitted: 11 March 2009
Accepted: 30 July 2009

REFERENCES

Akira, S., and K. Takeda. 2004. Toll-like receptor signalling. *Nat. Rev. Immunol.* 4:499–511.

Basu, S., A.R. Dunn, M.W. Marino, H. Savoia, G. Hodgson, G.J. Lieschke, and J. Cebon. 1997. Increased tolerance to endotoxin by granulocyte-macrophage colony-stimulating factor-deficient mice. *J. Immunol.* 159:1412–1417.

Bettelli, E., Y. Carrier, W. Gao, T. Korn, T.B. Strom, M. Oukka, H.L. Weiner, and V.K. Kuchroo. 2006. Reciprocal developmental pathways for the generation of pathogenic effector TH17 and regulatory T cells. *Nature.* 441:235–238.

Beutler, B., and E.T. Rietschel. 2003. Innate immune sensing and its roots: the story of endotoxin. *Nat. Rev. Immunol.* 3:169–176.

Bonnesen, C., I.M. Eggleston, and J.D. Hayes. 2001. Dietary indoles and isothiocyanates that are generated from cruciferous vegetables can both stimulate apoptosis and confer protection against DNA damage in human colon cell lines. *Cancer Res.* 61:6120–6130.

Brown, K., S. Park, T. Kanno, G. Franzoso, and U. Siebenlist. 1993. Mutual regulation of the transcriptional activator NF-kappa B and its inhibitor, I kappa B-alpha. *Proc. Natl. Acad. Sci. USA.* 90:2532–2536.

Burbach, K.M., A. Poland, and C.A. Bradfield. 1992. Cloning of the Ah-receptor cDNA reveals a distinctive ligand-activated transcription factor. *Proc. Natl. Acad. Sci. USA.* 89:8185–8189.

Burns, K., S. Janssens, B. Brissoni, N. Olivos, R. Beyaert, and J. Tschopp. 2003. Inhibition of interleukin 1 receptor/Toll-like receptor signaling through the alternatively spliced, short form of MyD88 is due to its failure to recruit IRAK-4. *J. Exp. Med.* 197:263–268.

Dragan, Y.P., and D. Schrenk. 2000. Animal studies addressing the carcinogenicity of TCDD (or related compounds) with an emphasis on tumour promotion. *Food Addit. Contam.* 17:289–302.

Ema, M., K. Sogawa, N. Watanabe, Y. Chujoh, N. Matsushita, O. Gotoh, Y. Funae, and Y. Fujii-Kuriyama. 1992. cDNA cloning and structure of mouse putative Ah receptor. *Biochem. Biophys. Res. Commun.* 184:246–253.

Fitzgerald, K.A., D.C. Rowe, B.J. Barnes, D.R. Caffrey, A. Visintin, E. Latz, B. Monks, P.M. Pitha, and D.T. Golenbock. 2003. LPS-TLR4 signaling to IRF-3/7 and NF-kappaB involves the toll adapters TRAM and TRIF. *J. Exp. Med.* 198:1043–1055.

Fujii-Kuriyama, Y., M. Ema, J. Miura, and K. Sogawa. 1994. Ah receptor: a novel ligand-activated transcription factor. *Exp. Clin. Immunogenet.* 1:65–74.

Funatake, C.J., N.B. Marshall, L.B. Steppan, D.V. Mourich, and N.I. Kerkvliet. 2005. Cutting edge: activation of the aryl hydrocarbon receptor by 2,3,7,8-tetrachlorodibenzo-p-dioxin generates a population of CD4+ CD25+ cells with characteristics of regulatory T cells. *J. Immunol.* 175:4184–4188.

Kanno, Y., Y. Takane, Y. Takizawa, and Y. Inouye. 2008. Suppressive effect of aryl hydrocarbon receptor repressor on transcriptional activity of estrogen receptor alpha by protein–protein interaction in stably and transiently expressing cell lines. *Mol. Cell. Endocrinol.* 291:87–94.

Karaghiosoff, M., R. Steinborn, P. Kovarik, G. Kriegshäuser, M. Baccarini, B. Donabauer, U. Reichart, T. Kolbe, C. Bogdan, T. Leanderson, et al. 2003. Central role for type I interferons and Tyk2 in lipopolysaccharide-induced endotoxin shock. *Nat. Immunol.* 4:471–477.

Kawai, T., O. Adachi, T. Ogawa, K. Takeda, and S. Akira. 1999. Unresponsiveness of MyD88-deficient mice to endotoxin. *Immunity.* 11:115–122.

Kimura, A., T. Naka, T. Muta, O. Takeuchi, S. Akira, I. Kawase, and T. Kishimoto. 2005. Suppressor of cytokine signaling-1 selectively inhibits LPS-induced IL-6 production by regulating JAK-STAT. *Proc. Natl. Acad. Sci. USA.* 102:17089–17094.

Kimura, A., T. Naka, K. Nohara, Y. Fujii-Kuriyama, and T. Kishimoto. 2008. Aryl hydrocarbon receptor regulates Stat1 activation and participates in the development of Th17 cells. *Proc. Natl. Acad. Sci. USA.* 105:9721–9726.

Moore, K.W., R. de Waal Malefyt, R.L. Coffman, and A. O'Garra. 2001. Interleukin-10 and the interleukin-10 receptor. *Annu. Rev. Immunol.* 19:683–765.

Naiki, Y., K.S. Michelsen, W. Zhang, S. Chen, T.M. Doherty, and M. Arditi. 2005. Transforming growth factor-beta differentially inhibits MyD88-dependent, but not TRAM- and TRIF-dependent, lipopolysaccharide-induced TLR4 signaling. *J. Biol. Chem.* 280:5491–5495.

Nakagawa, R., T. Naka, H. Tsutsui, M. Fujimoto, A. Kimura, T. Abe, E. Seki, S. Sato, O. Takeuchi, K. Takeda, et al. 2002. SOCS-1 participates in negative regulation of LPS responses. *Immunity.* 17:677–687.

Negishi, T., Y. Kato, O. Ooneda, J. Mimura, T. Takada, H. Mochizuki, M. Yamamoto, Y. Fujii-Kuriyama, and S. Furusako. 2005. Effects of aryl hydrocarbon receptor signaling on the modulation of TH1/TH2 balance. *J. Immunol.* 175:7348–7356.

Ohtake, F., K. Takeyama, T. Matsumoto, H. Kitagawa, Y. Yamamoto, K. Nohara, C. Tohyama, A. Krust, J. Mimura, P. Chambon, et al. 2003. Modulation of oestrogen receptor signalling by association with the activated dioxin receptor. *Nature.* 423:545–550.

Ohtake, F., A. Baba, I. Takada, M. Okada, K. Iwasaki, H. Miki, S. Takahashi, A. Kouzmenko, K. Nohara, T. Chiba, et al. 2007. Dioxin receptor is a ligand-dependent E3 ubiquitin ligase. *Nature.* 446:562–566.

Puga, A., S.J. Barnes, T.P. Dalton, C. Chang, E.S. Knudsen, and M.A. Maier. 2000. Aromatic hydrocarbon receptor interaction with the retinoblastoma protein potentiates repression of E2F-dependent transcription and cell cycle arrest. *J. Biol. Chem.* 275:2943–2950.

Puga, A., C.R. Tomlinson, and Y. Xia. 2005. Ah receptor signals cross-talk with multiple developmental pathways. *Biochem. Pharmacol.* 69:199–207.

Quintana, F.J., A.S. Basso, A.H. Iglesias, T. Korn, M.F. Farez, E. Bettelli, M. Caccamo, M. Oukka, and H.L. Weiner. 2008. Control of T(reg) and T(H)17 cell differentiation by the aryl hydrocarbon receptor. *Nature.* 453:65–71.

Shimizu, Y., Y. Nakatsuru, M. Ichinose, Y. Takahashi, H. Kume, J. Mimura, Y. Fujii-Kuriyama, and T. Ishikawa. 2000. Benzo[a]pyrene carcinogenicity is lost in mice lacking the aryl hydrocarbon receptor. *Proc. Natl. Acad. Sci. USA.* 97:779–782.

Stumhofer, J.S., A. Laurence, E.H. Wilson, E. Huang, C.M. Tato, L.M. Johnson, A.V. Villarino, Q. Huang, A. Yoshimura, D. Sehy, et al. 2006. Interleukin 27 negatively regulates the development of interleukin 17-producing T helper cells during chronic inflammation of the central nervous system. *Nat. Immunol.* 7:937–945.

Tian, Y., S. Ke, M.S. Denison, A.B. Rabson, and M.A. Gallo. 1999. Ah receptor and NF-kappaB interactions, a potential mechanism for dioxin toxicity. *J. Biol. Chem.* 274:510–515.

Tian, Y., A.B. Rabson, and M.A. Gallo. 2002. Ah receptor and NF-kappaB interactions: mechanisms and physiological implications. *Chem. Biol. Interact.* 141:97–115.

Toshchakov, V., B.W. Jones, P.Y. Perera, K. Thomas, M.J. Cody, S. Zhang, B.R. Williams, J. Major, T.A. Hamilton, M.J. Fenton, and S.N. Vogel. 2002. TLR4, but not TLR2, mediates IFN-beta-induced STAT1alpha/beta-dependent gene expression in macrophages. *Nat. Immunol.* 3:392–398.

Veldhoen, M., K. Hirota, A.M. Westendorf, J. Buer, L. Dumoutier, J.C. Renauld, and B. Stockinger. 2008. The aryl hydrocarbon receptor links TH17-cell-mediated autoimmunity to environmental toxins. *Nature.* 453:106–109.

Veldhoen, M., K. Hirota, J. Christensen, A. O'Garra, and B. Stockinger. 2009. Natural agonists for aryl hydrocarbon receptor in culture medium are essential for optimal differentiation of Th17 T cells. *J. Exp. Med.* 206:43–49.

Vogel, C.F., E. Sciullo, W. Li, P. Wong, G. Lazennec, and F. Matsumura. 2007. RelB, a new partner of aryl hydrocarbon receptor-mediated transcription. *Mol. Endocrinol.* 21:2941–2955.

Yamamoto, M., S. Yamazaki, S. Uematsu, S. Sato, H. Hemmi, K. Hoshino, T. Kaisho, H. Kuwata, O. Takeuchi, K. Takeshige, et al. 2004. Regulation of Toll/IL-1-receptor-mediated gene expression by the inducible nuclear protein IkappaBzeta. *Nature.* 430:218–222.

Yoshimura, A., T. Naka, and M. Kubo. 2007. SOCS proteins, cytokine signalling and immune regulation. *Nat. Rev. Immunol.* 7:454–465.

Published

SUPPLEMENTAL MATERIAL

Kimura et al., http://www.jem.org/cgi/content/full/jem.20090560/DC1

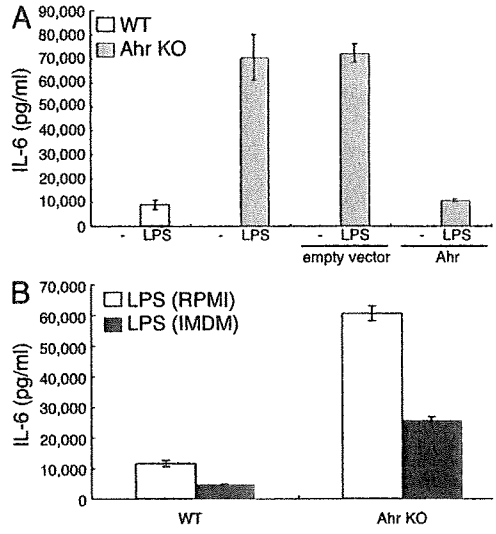

Figure S1. Ahr regulates LPS-induced IL-6 production independently on culture medium. (A) Ahr-deficient cells were transduced with Ahr-encoding retrovirus. WT, Ahr KO cells, and Ahr KO cells transduced with Ahr were stimulated with LPS for 24 h. The production of IL-6 was measured by means of ELISA. Data show means ± SEM of three independent experiments. (B) WT and Ahr KO peritoneal macrophages cultured in RPMI or IMDM medium were stimulated with LPS for 24 h. The production of IL-6 was measured by means of ELISA. Data show means ± SEM of three independent experiments.

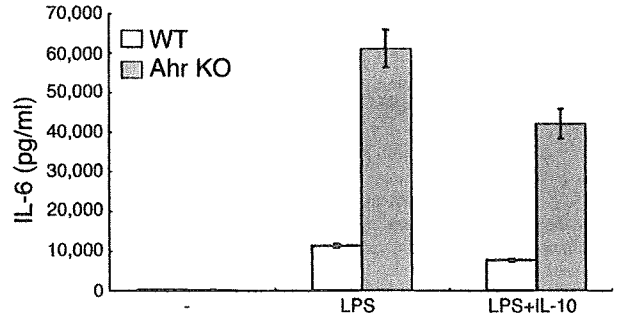

Figure S2. Ahr regulates LPS-induced IL-6 production independently of IL-10. WT and Ahr KO peritoneal macrophages were stimulated with LPS in the presence or absence of IL-10 for 24 h. The production of IL-6 was measured by means of ELISA. Data show means ± SEM of three independent experiments.

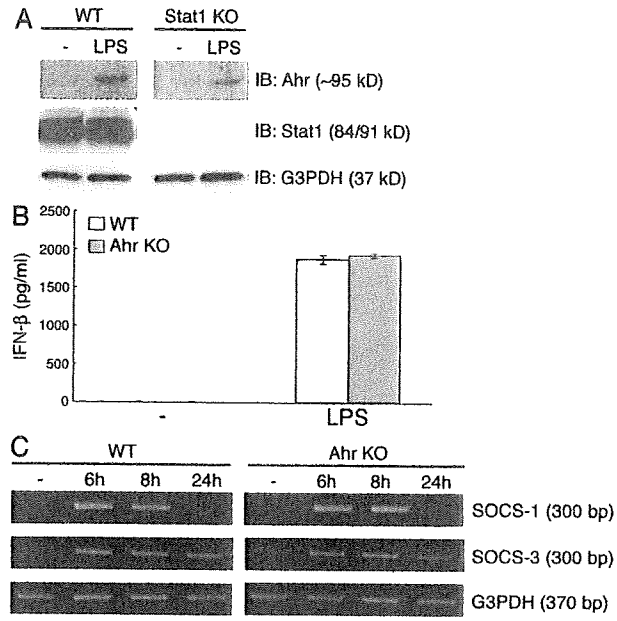

Figure S3. Normal induction of Ahr in Stat1-deficient peritoneal macrophages and IFN-β and SOCS family members in Ahr KO cells. (A) WT and Stat1 KO peritoneal macrophages were stimulated with LPS for 24 h. The cells were lysed and subjected to immunoblotting (IB) analysis for the expression of Ahr and G3PDH. Data are from one representative of three independent experiments. (B) Peritoneal macrophages from WT and Ahr KO mice were stimulated with LPS for 24 h. The production of IFN-β was measured by means of ELISA. Data show means ± SEM of three independent experiments. (C) Peritoneal macrophages from WT and Ahr KO mice were stimulated with LPS for the indicated periods of time. Total RNA and cDNA were prepared after LPS stimulation. SOCS-1 and SOCS-3 induction was examined by using reverse transcription-PCR. Data are from one representative of three independent experiments.

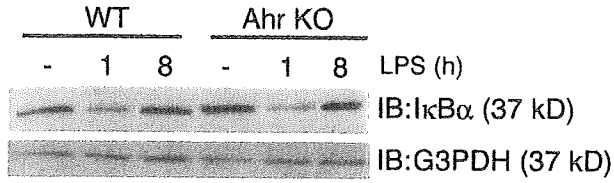

Figure S4. There is no difference in IκBα degradation by LPS between WT and Ahr KO peritoneal macrophages. WT and Ahr KO peritoneal macrophages were stimulated with LPS for the indicated periods of time. Cells were lysed and whole cell lysates were used for immunoblotting analysis with anti-IκBα and anti-G3PDH antibodies. Data are from one representative of three independent experiments.

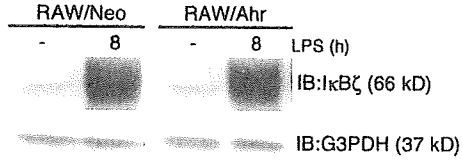

Figure S5. IκBζ is induced by LPS in the presence or absence of Ahr. RAW/Neo and RAW/Ahr were stimulated with LPS for 8 h Cells were lysed and whole cell lysates were used for immunoblotting analysis with anti-IκBζ and anti-G3PDH Abs. Data are from one representative of three independent experiments.

Aryl hydrocarbon receptor suppresses intestinal carcinogenesis in $Apc^{Min/+}$ mice with natural ligands

Kaname Kawajiri[a,1], Yasuhito Kobayashi[b], Fumiaki Ohtake[c,d], Togo Ikuta[a], Yoshibumi Matsushima[a], Junsei Mimura[e], Sven Pettersson[f], Richard S. Pollenz[g], Toshiyuki Sakaki[h], Takatsugu Hirokawa[i], Tetsu Akiyama[d], Masafumi Kurosumi[b], Lorenz Poellinger[j], Shigeaki Kato[c,d], and Yoshiaki Fujii-Kuriyama[c,e]

[a]Research Institute for Clinical Oncology and [b]Hospital, Saitama Cancer Center, 818 Komuro, Ina, Saitama, 362-0806, Japan; [c]Exploratory Research for Advanced Technology and Solution Oriented Research for Science and Technology, Japan Science and Technology Agency, 4-1-8 Honcho, Kawaguchi, Saitama, 332-0012, Japan; [d]Institute of Molecular and Cellular Biosciences, University of Tokyo, 1-1-1 Yayoi, Bunkyo-ku, Tokyo, 113-0032, Japan; [e]Tsukuba Advanced Research Alliance Center, University of Tsukuba, Tennodai, Tsukuba, Ibaraki, 305-8577, Japan; [f]Germ-Free Facility and [j]Department of Cell and Molecular Biology, Karolinska Institute, S-171 77 Stockholm, Sweden; [g]Department of Biology, University of South Florida, Tampa, FL 33620; [h]Department of Biotechnology, Toyama Prefectural University, 5180 Kurokawa, Imizu, Toyama, 939-0398, Japan; and [i]Computational Biology Research Center, National Institute of Advanced Industrial Science and Technology, 2-42 Aomi, Koto-ku, Tokyo, 135-0064, Japan

Edited by Tadatsugu Taniguchi, University of Tokyo, Tokyo, Japan, and approved June 23, 2009 (received for review February 26, 2009)

Intestinal cancer is one of the most common human cancers. Aberrant activation of the canonical Wnt signaling cascade, for example, caused by adenomatous polyposis coli (APC) gene mutations, leads to increased stabilization and accumulation of β-catenin, resulting in initiation of intestinal carcinogenesis. The aryl hydrocarbon receptor (AhR) has dual roles in regulating intracellular protein levels both as a ligand-activated transcription factor and as a ligand-dependent E3 ubiquitin ligase. Here, we show that the AhR E3 ubiquitin ligase has a role in suppression of intestinal carcinogenesis by a previously undescribed ligand-dependent β-catenin degradation pathway that is independent of and parallel to the APC system. This function of AhR is activated by both xenobiotics and natural AhR ligands, such as indole derivatives that are converted from dietary tryptophan and glucosinolates by intestinal microbes, and suppresses intestinal tumor development in $Apc^{Min/+}$ mice. These findings suggest that chemoprevention with naturally-occurring and chemically-designed AhR ligands can be used to successfully prevent intestinal cancers.

cecal cancer | ubiquitin ligase | β-catenin | tumor chemoprevention

The aryl hydrocarbon receptor (AhR, also known as dioxin receptor) is a member of a transcription factor superfamily that is characterized by structural motifs of basic helix–loop–helix (bHLH)/Per-AhR nuclear translocator (Arnt)-Sim (PAS) domains, and also includes hypoxia-inducible factors (HIFs). Over the past decade, many studies have been focused on elucidating the functions of AhR as a mediator of multiple pharmacological and toxicological effects such as the induction of drug-metabolizing enzymes, teratogenesis, tumor promotion, and immunosuppression caused by environmental contaminants such as 3-methylcholanthrene (MC) and 2,3,7,8-tetrachlorodibenzo-*p*-dioxin (TCDD) (1, 2). On ligand binding, AhR translocates from the cytoplasm into the nucleus where it heterodimerizes with the Arnt and activates the transcription of target genes such as *Cyp1a1*. Induction of the *Cyp1a1* gene leads to the biotransformation of polycyclic aromatic hydrocarbons into active genotoxic metabolites, resulting in the initiation of chemical carcinogenesis (3). AhR-deficient ($AhR^{-/-}$) mice are resistant to most, if not all, of these toxicological adverse effects, indicating that AhR is a key factor in the development of these chemical-induced diseases (4, 5). Also, we recently found that AhR functions as a ligand-dependent E3 ubiquitin ligase of certain nuclear receptors (6), such as the estrogen (ER) and androgen receptors (AR). Most recently, AhR has been reported to have a crucial role in the differentiation of regulatory T cells (7–9).

AhR is a nucleocytoplasmic shuttling protein, the intracellular localization of which is changed depending on cell density in the absence of exogenous ligands (10). Such cell density-dependent movements between the cytoplasm and nucleus have also been reported for some tumor suppressor gene products, such as VHL (11) and adenomatous polyposis coli (APC) (12). Also, the natural AhR ligands of indole derivatives (13, 14), such as indole-3-acetic acid (IAA, so-called plant auxin), indole-3-carbinol (I3C) and 3,3′-diindolylmethane (DIM), are natural AhR ligands and generated through conversion from dietary tryptophan (Trp) and glucosinolates, respectively, by commensal intestinal microbes (15). Notably, glucosinolates have been reported to exert the chemopreventive effects on colorectal cancers in humans by cruciferous vegetables (16–18). Together, these lines of evidence suggest that AhR has some functional association with intestinal carcinogenesis.

Results

Cecal Tumor Development in $AhR^{-/-}$ Mice. After thoroughly examining the digestive tracts of $AhR^{-/-}$ mice, we found that $AhR^{-/-}$ mice, but not heterozygous $AhR^{+/-}$ or wild-type $AhR^{+/+}$ mice, frequently developed colonic tumors, mostly in the cecum near the ileocecal junction (Fig. 1 *A* and *B*). $AhR^{-/-}$ mice bred at 2 independent animal houses showed a similar time course of macroscopic tumor incidence (Fig. S1*B*), and the tumor size increased gradually by age, reached a plateau at ≈30 to 40 weeks (Fig. 1*B*). To date, 3 independent $AhR^{-/-}$ mice lines have been reported (4, 19, 20). Although one report described frequent rectal prolapse (Fig. S1*A*) and marked colonic hyperplasia with severe inflammation in $AhR^{-/-}$ mice (19), there have been no systematic studies on intestinal carcinogenesis, which may explain why the tumor suppressor function of AhR has been unreported to date. Colorectal cancer is one of the most common human cancers, 5–10% of which originates in the cecum. Therefore, we were interested in investigating how $AhR^{-/-}$ mice develop spontaneous cecal tumors.

Randomly selected mice were examined histologically for atypia classified according to the standards as shown in Fig. S2. Although $AhR^{+/+}$ and $AhR^{+/-}$ mice of all ages had normal (Grade 1) to mild hyperplasia (Grade 2) at worst, $AhR^{-/-}$ mice older than 11 weeks had abnormal histology with atypia ranging from mild malignancy of polyps to severe carcinomas that were exacerbated with age (Fig. 1*C*). Close microscopic examination revealed that the $AhR^{-/-}$ mice bore cecal lesions with a mod-

Author contributions: K.K., S.K., and Y.F.-K. designed research; K.K., Y.K., F.O., T.I., Y.M., J.M., S.P., T.S., T.H., M.K., and L.P. performed research; R.S.P. and T.A. contributed new reagents/analytic tools; K.K., L.P., S.K., and Y.F.-K. analyzed data; and K.K., L.P., and Y.F.-K. wrote the paper.

The authors declare no conflict of interest.

This article is a PNAS Direct Submission.

[1]To whom correspondence should be addressed. E-mail: kawajiri@cancer-c.pref.saitama.jp.

This article contains supporting information online at www.pnas.org/cgi/content/full/0902132106/DCSupplemental.

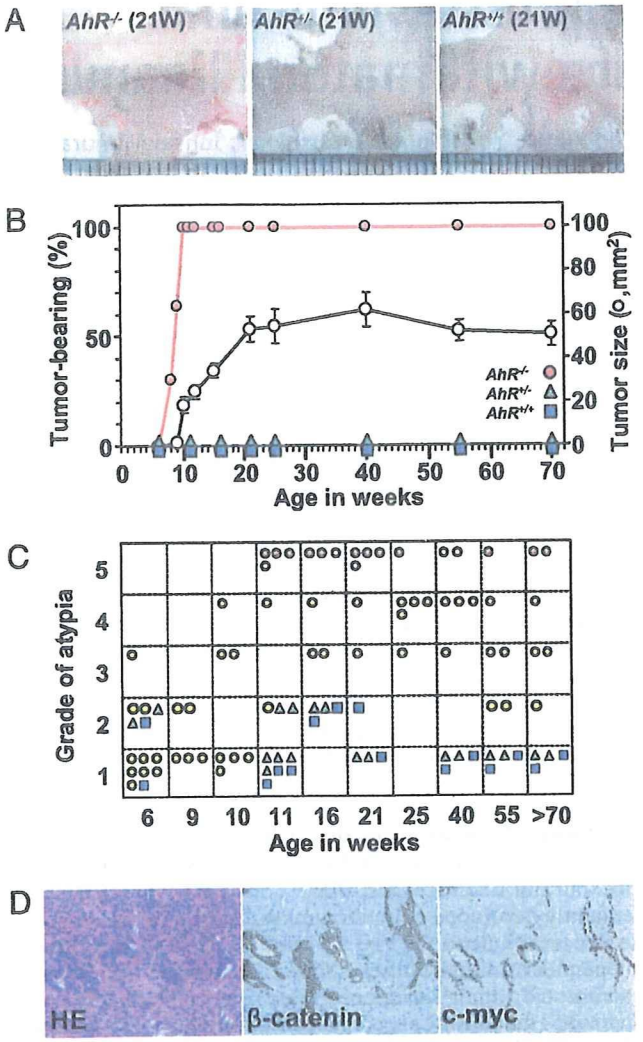

Fig. 1. Cecal tumor development in $AhR^{-/-}$ mice. (*A*) Representative profiles of colon tumors at the cecum in $AhR^{-/-}$ mice. (*B*) Relationship between the time course of macroscopic tumor incidence and tumor growth by age. Tumor size was estimated based on NIH images as shown by beige circles. Error bars, means ± SD. (*C*) Summary of histological atypia grades of tumors in $AhR^{-/-}$ mice by age. $AhR^{+/+}$ (blue squares), $AhR^{+/-}$ (green triangles), and $AhR^{-/-}$ (yellow circles) are shown. $AhR^{-/-}$ mice with adenocarcinomas (Grade 5) that had invaded the submucosal region or beyond (red circles) and within the intramucosal region (pink circles) are shown separately. (*D*) Representative H&E staining profile of a moderately differentiated adenocarcinoma and immunohistochemical staining with an antibody against β-catenin or c-myc.

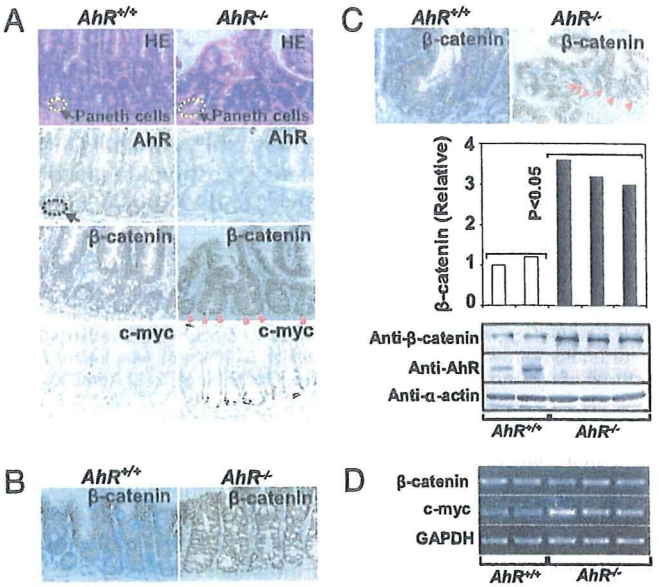

Fig. 2. Abnormal β-catenin accumulation in the intestines of $AhR^{-/-}$ mice. (*A*) H&E staining and immunohistochemical staining of mouse small intestines. Paneth cells were observed at the bottom of the crypts in the small intestine in both genotypes. Expression of AhR, β-catenin, and c-myc are shown. Nuclear accumulation of β-catenin in Paneth cells of the small intestine and cecum is noted by red arrowheads. Immunohistochemical staining of β-catenin in the colons (*B*) or cecum (*C*) of $AhR^{+/+}$ or $AhR^{-/-}$ mice. (*C*) Levels of β-catenin, AhR and α-actin in the cecum were detected by Western blotting. The amount of β-catenin was quantified using the ImageJ software (NIH). ($P < 0.05$; $AhR^{+/+}$ versus $AhR^{-/-}$ group). (*D*) RT-PCR was performed to detect mRNA levels for β-catenin, c-myc ($P < 0.05$; $AhR^{+/+}$ versus $AhR^{-/-}$ group), and GAPDH in the cecal epithelium of $AhR^{+/+}$ or $AhR^{-/-}$ mice. Data are representative of 3 independent experiments.

erate (Grade 3: 9/42) or a high grade of atypia, adenoma (Grade 4: 12/42), and adenocarcinoma (Grade 5: 17/42). Among the 17 diagnosed adenocarcinomas, 12 tumors (71%) invaded the submucosal region or beyond, and the remainder were located within the intramucosal region. Overall survival rates estimated by the Kaplan-Meyer method (Fig. S1*C*) revealed that $AhR^{-/-}$ mice had a significantly shorter lifespan than wild-type or heterozygous mice (log-rank test; $P = 4.4 \times 10^{-9}$), although this shorter longevity might not be only due to cecal tumors in the $AhR^{-/-}$ mice (19).

The detected cecal cancers were predominantly tubular adenocarcinomas with various degrees of malignancy (Fig. S3). A representative profile of moderately differentiated adenocarcinomas with irregularly shaped and fused tubular structures that sometimes invaded the submucosal regions is presented in Fig. 1*D*. In these cells, immunohistochemical staining showed concomitant overexpression of β-catenin and c-myc, a target gene of β-catenin/TCF4 (21). It remains uninvestigated whether there should occur any further genetic alterations in $AhR^{-/-}$ mice leading to carcinogenesis. In human cecal cancers, markedly reduced expression of AhR was also found concomitantly with an abnormal accumulation of β-catenin in all of 12 cancer specimens from our hospital (Fig. S4).

The β-Catenin Accumulation in $AhR^{-/-}$ Mice. To examine the molecular mechanism underlying tumor development in $AhR^{-/-}$ mice, we analyzed the expression of both AhR and β-catenin in the intestines of 6-week-old $AhR^{+/+}$ and $AhR^{-/-}$ mice, which had a morphologically normal epithelium. AhR expression was relatively abundant in Paneth cells (22), which have a host-defensive role against microbes in the small intestine and the cecum in $AhR^{+/+}$ mice, but was undetectable in $AhR^{-/-}$ mice (Fig. 2*A*). Significant AhR expression was also observed in Paneth cells of the small intestine and the cecum in humans (Fig. S5). Notably, β-catenin expression was abnormally high in epithelial cells of the ileum (Fig. 2*A*), colon (Fig. 2*B*), and cecum (Fig. 2*C*) in $AhR^{-/-}$ mice, suggesting that the intestines of $AhR^{-/-}$ mice may be in a "cancer-prone" or "precancerous" state (23). In particular, these elevated levels of β-catenin were observed in the nuclei of Paneth cells compared with the corresponding regions in wild-type mice (Fig. 2*A*).

Using Western blotting (Fig. 2*C*), we confirmed that $AhR^{-/-}$ mice had significantly higher levels of β-catenin in the cecum than wild-type mice ($P < 0.05$), whereas β-catenin mRNA expression levels were unchanged (Fig. 2*D*), suggesting that the stabilization, but not enhanced synthesis of the β-catenin protein in the $AhR^{-/-}$ intestine leads to β-catenin accumulation. Con-

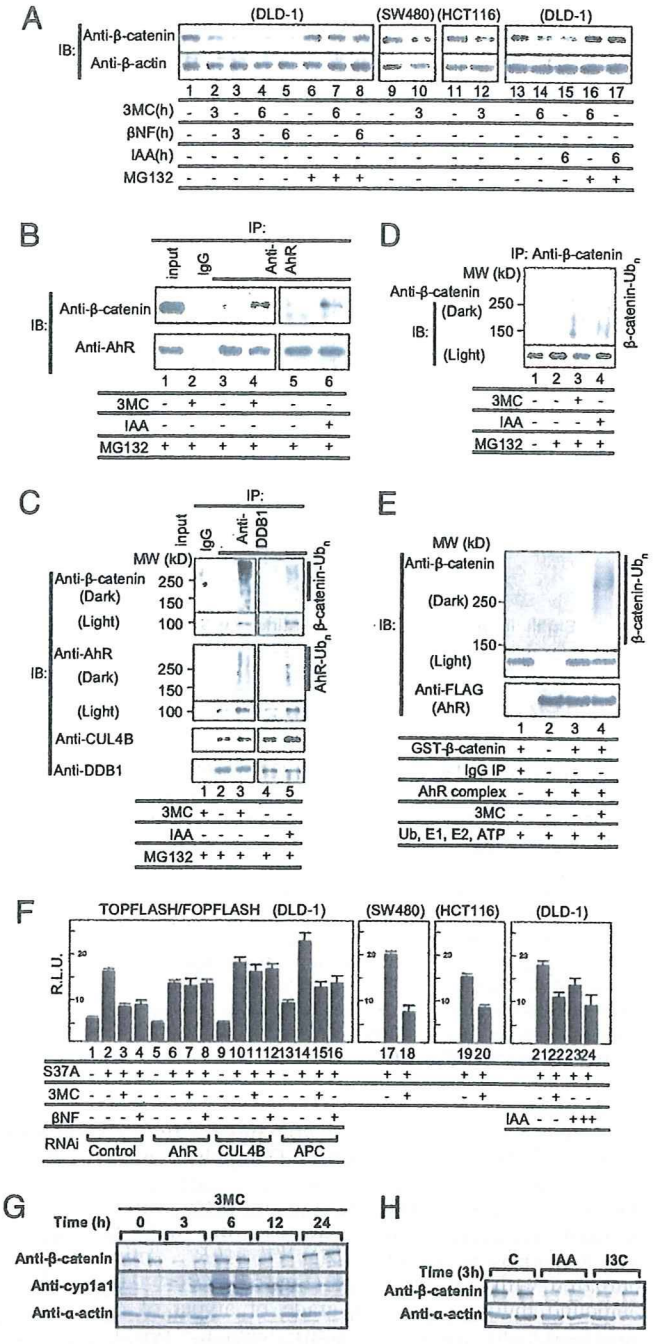

Fig. 3. Novel AhR ligand-dependent ubiquitylation and proteasomal degradation of β-catenin. (*A*) Activated AhR promotes proteasomal degradation of β-catenin. Cells were incubated as indicated with 3MC (1 μM), βNF (1 μM), or IAA (100 μM) in the presence or absence of the proteasome inhibitor MG132 (10 μM) for 3 or 6 h. Cell lysates were subjected to Western blotting with antibodies indicated. (*B*) Ligand-dependent recognition of β-catenin by AhR. DLD-1 cells were incubated with 3MC or IAA and MG132 for 2 h. Then, the extracts were prepared and immunoprecipitated. (*C*) Ligand-dependent complex assembly of CUL4B^{AhR} E3 ligase with β-catenin. DLD-1 cells were incubated with 3MC or IAA and MG132 for 2 h, after which the cell extracts were prepared and immunoprecipitated with an anti-DDB1 antibody to detect CUL4B^{AhR} complexes with β-catenin. Western blottings were subjected to a long exposure (Dark) to detect polyubiquitylated forms of the proteins. (*D*) AhR ligand-induced ubiquitylation of β-catenin. DLD-1 cells were incubated with the indicated ligands and MG-132 for 6 h. (*E*) The AhR complex directly ubiquitylates β-catenin in vitro. The FLAG-HA-AhR-associated immunocomplex in the presence of CUL4B^{AhR} components was mixed with recombinant GST-β-catenin (Fig. S6*D*) and His-ubiquitin, and an in vitro ubiquitylation assay was performed. (*F*) CUL4B^{AhR} components are essential for AhR ligand-dependent repression of hyperactive β-catenin (S37A) transactivation. Cells were incubated as indicated with 3MC (1 μM), βNF (1 μM), or IAA (+, 10 μM; ++, 100 μM). All values are means ± SD for at least 3 independent experiments. (*G*) AhR ligand-dependent β-catenin degradation in vivo. AhR$^{+/+}$ mice received a single i.p. injection of 3MC (4 mg/kg). The levels of proteins in the cecal epithelium were determined. (*H*) *AhR*$^{+/+}$ mice received a single i.p. injection of IAA or I3C (25 mg/kg).

sistent with the abnormal accumulation of β-catenin, expression of the downstream target, c-myc, showed ≈2-fold induction (Fig. 2 *A* and *D*).

Ligand-Dependent Degradation of β-Catenin. Next, we examined whether the AhR E3 ubiquitin ligase participates in the degradation of β-catenin (Fig. 3) as reported (6) for the degradation of ER and AR. On activation of AhR by exogenous ligands, 3MC or β-naphthoflavone (βNF), endogenous β-catenin protein levels markedly decreased in DLD-1 cells derived from a colon cancer and in other colon cancer-derived cells, SW480 and HCT116 (Fig. 3*A*). These results clearly show that β-catenin is degraded in an AhR ligand-dependent manner even in colon cancer-derived cells harboring mutations (24) in *APC* or *β-catenin* that stabilize β-catenin protein against APC-dependent degradation. These findings suggest that AhR participates in a previously undescribed mechanism of β-catenin degradation that is independent of the APC pathway. Also, after the addition of IAA, which is produced in the intestine from Trp by intestinal microbes (15), and was detected in the cecal contents by HPLC (Fig. S6*H*), AhR-dependent degradation of β-catenin was also observed (Fig. 3*A*; Fig. S6*A*). Degradation of β-catenin induced by xenobiotics or natural AhR ligands was abrogated in the presence of either the proteasome inhibitor MG132 (Fig. 3*A*) or AhR siRNA (Fig. S6*A*). We observed that the AhR ligands promoted selective degradation of β-catenin in the soluble fractions, but not in the membrane fraction of cells (Fig. S6*B*), suggesting that β-catenin involved in the Wnt signaling pathway is selectively degraded. Recognition of endogenous β-catenin by AhR was clearly ligand-dependent, as shown by coimmunoprecipitation assays (Fig. 3*B*). Also, AhR ligand-dependent assembly of the Cullin (CUL)4B^{AhR} E3 ligase complex with β-catenin (Fig. 3*C*) was detected by immunoprecipitation assays using an antibody to DDB1 (6), a component of the E3 ubiquitin ligase complex of AhR, together with ligand-induced polyubiquitylation of β-catenin (Fig. 3 *C* and *D*) and self-ubiquitylation of AhR (Fig. 3*C*). AhR-mediated degradation of β-catenin was reconstituted in an in vitro ubiquitylation assay. In this assay, immunopurified CUL4B^{AhR} complexes showed, as expected, E3 ubiquitin ligase activity toward ER (Fig. S6*C*) and purified GST-β-catenin (Fig. 3*E*; Fig. S6*D*). In both these cases, the E3 ubiquitin ligase activity was increased by addition of the ligand, 3MC (Fig. 3*E*; Fig. S6*C*). These data strongly suggest that the ligand-dependent E3 ubiquitin ligase activity of AhR participates in β-catenin degradation, and is consistent with the repression of the transcriptional activity of endogenous β-catenin by 3MC (Fig. S6*E*).

To substantiate AhR-dependent degradation of β-catenin in terms of its transcriptional activity and its relationship with the canonical APC-dependent degradation system, we performed reporter assays with TOPFLASH/FOPFLASH mediated by a hyperactive β-catenin (S37A) mutant (Fig. 3*F*) (25). The reporter activity was enhanced by the addition of β-catenin, and the enhanced reporter expression was repressed by the AhR ligands, 3MC, βNF, and IAA ($P < 0.05$). Repression of the transcriptional activity of β-catenin by AhR ligands was reversed by AhR or CUL4B siRNA, but not by APC siRNA, confirming that AhR is involved in a previously undescribed ligand-dependent mechanism of proteasomal degradation of β-catenin

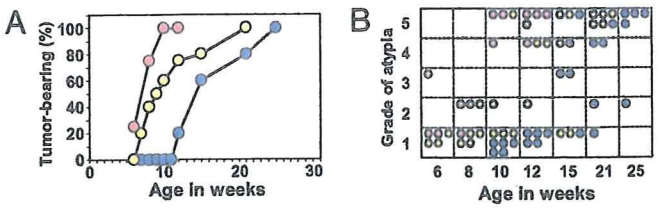

Fig. 4. Functional cooperation between Apc and AhR with regard to cecal tumor incidence. Macroscopic cecal tumor incidence by age in weeks (*A*) and summary of histological grades of atypia (*B*) that developed in $Apc^{Min/+}$·$AhR^{+/+}$ (blue circles), $Apc^{Min/+}$·$AhR^{+/-}$ (yellow circles), and $Apc^{Min/+}$·$AhR^{-/-}$ (red circles) mice. Four to 5 mice were used in each group.

that is distinct from the canonical APC-dependent pathway (Fig. 3*F*; Fig. S6*F*).

We were interested to investigate whether β-catenin protein is reduced in vivo in the intestines of mice after AhR ligand treatment. AhR ligand-dependent degradation of the β-catenin protein was clearly observed in vivo in the intestines of mice with a peak at 3 h after i.p. injection of 3MC, whereas cyp1a1 expression was markedly enhanced as expected (Fig. 3*G*). This transient degradation of β-catenin is likely due to the rapid down-regulation of AhR after ligand activation (6). Also, this in vivo degradation of β-catenin by 3MC was AhR-dependent, because accumulated β-catenin levels in the cecal epithelia of $AhR^{-/-}$ mice were not altered by 3MC treatment (Fig. S6*G*). Also, in vivo degradation of β-catenin was observed after i.p. injection of the natural AhR ligands, IAA and I3C (Fig. 3*H*). HPLC analysis of cecal materials demonstrated that the production of natural AhR ligands [IAA (≈1.2 μM), TA (tryptamin) (≈7.2 μM), and indole (≈43 μM)] depended on the presence of intestinal microbes (Fig. S6*H*), and the concentrations of these ligands were in a range that effectively activates AhR. During 3MC treatment, β-catenin mRNA levels remained unchanged with a slight, but reproducible decrease in c-myc mRNA expression, whereas cyp1a1 mRNA levels were markedly enhanced (Fig. S6*I*). These in vivo observations are highly consistent with the in vitro experiments, and provide a basis for possible chemoprevention against intestinal carcinogenesis by using natural AhR ligands.

Cooperative Function Between Apc and AhR Pathways. The tumor suppressor *APC* gene was originally discovered as a gene responsible for a hereditary cancer syndrome termed familial adenomatous polyposis (FAP) (26, 27). *APC* mutations are also found in most sporadic colorectal cancers (28) with an abnormal accumulation of β-catenin. The murine model of FAP, $Apc^{Min/+}$ (multiple intestinal neoplasia/+), carries an *Apc* mutation (29). However, in contrast to FAP patients who develop tumors in the colon (28), these mice develop numerous adenomatous polyps mostly in the small intestine, although the reasons for this difference remain unknown.

To investigate a functional association between the Apc- and AhR-mediated pathways of β-catenin degradation with regard to intestinal tumor development, we generated mice with compound mutations in both the *Apc* and *AhR* genes with the same genetic background. We observed no effect of AhR mutation on the expression of Apc, and vice versa (Fig. S7*A*). The tumor incidence in compound $Apc^{Min/+}$·*AhR*-disrupted mutant mice was compared with that of single gene mutant $Apc^{Min/+}$ mice. In the cecum (Fig. 4*A*), $Apc^{Min/+}$ mice showed a tumor incidence of ≈50% of the total at 14 weeks of age that reached 100% at 25 weeks of age, whereas no tumors were found in $AhR^{+/-}$ mice (Fig. 1*B*). Remarkably, the compound $Apc^{Min/+}$·$AhR^{+/-}$ mutant mice had a tumor incidence of 50% at 9–10 weeks of age, and were much more susceptible to cecal tumorigenesis than $Apc^{Min/+}$ mice, which supports a cooperative tumor suppression function between the 2 genes. Compound $Apc^{Min/+}$·$AhR^{-/-}$ mutant mice displayed this tendency more prominently, although in limited numbers because of difficulty in breeding. A similarly accelerated carcinogenesis in the small intestine at 7 and 8 weeks was observed in $Apc^{Min/+}$·$AhR^{+/-}$ mice (Fig. 5*D*) compared with $Apc^{Min/+}$ mice (Fig. 5*B*) ($P < 0.001$). In the compound mutant mice, the grade of atypia of cecal tumors progressed with age in a cooperative manner, reflecting a cooperative interaction between the AhR and Apc pathways (Fig. 4*B*).

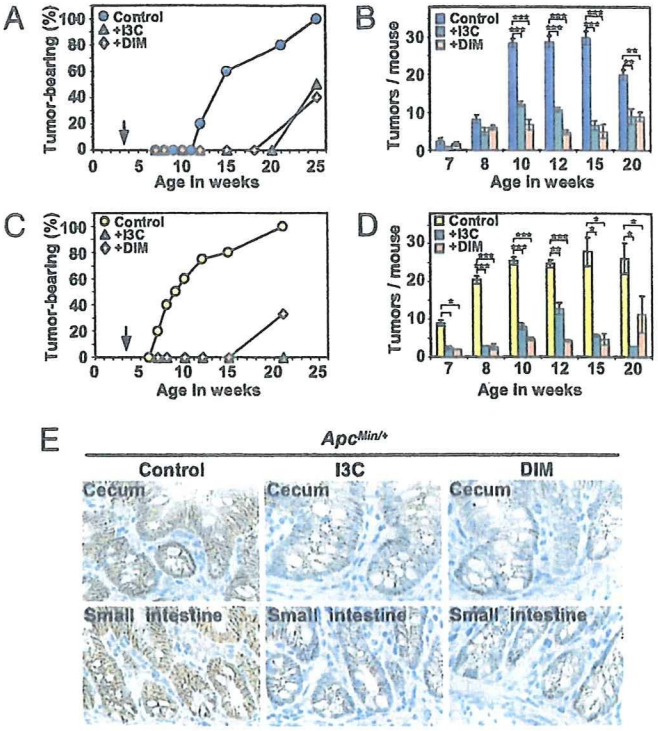

Fig. 5. Natural AhR ligands suppress intestinal carcinogenesis. Four to 5 mice were used in each group. Cecal carcinogenesis in the $Apc^{Min/+}$ (*A*) and $Apc^{Min/+}$·$AhR^{+/-}$ (*C*) mice. Tumor development in mice fed a control diet (blue circles in *A* and yellow circles in *C*), 0.1% I3C-containing (green triangles) or 0.01% DIM-containing (beige diamondes) diet just after weaning of 3–4 weeks of age as noted by the arrows. Number of small intestinal polyps in $Apc^{Min/+}$ (*B*, blue squares) or $Apc^{Min/+}$·$AhR^{+/-}$ (*D*, yellow squares) mice fed a control diet. Number of polyps in the small intestines of mice fed an I3C-containing (green squares) or DIM-containing (beige squares) diet. Data are presented as means ± SD. *, $P < 0.01$; **, $P < 0.001$; ***, $P < 0.0001$. (*E*) Representative profile of immunohistochemical staining with an antibody against β-catenin in the intestines from 15-week-old $Apc^{Min/+}$ mice fed a control or ligand-containing diet.

To determine how compound $Apc^{Min/+}$·*AhR*-disrupted mutant mice were more susceptible to cecal tumorigenesis than $Apc^{Min/+}$ mice, β-catenin levels were monitored in the cecum by Western blotting (Fig. S7*B*) and immunohistochemistry (Fig. S7*C*) at 6 to 8 weeks of age, when a morphologically normal epithelium was observed (Fig. 4*B*). And we found elevated levels of β-catenin in the cecum of both $Apc^{Min/+}$·$AhR^{-/-}$ and $Apc^{Min/+}$·$AhR^{+/-}$ mice compared with $Apc^{Min/+}$·$AhR^{+/+}$ mice, suggesting an association between the levels of β-catenin and tumor susceptibility. Expression levels of the β-catenin/TCF4 target genes, c-myc and cyclin D1, were concomitantly enhanced in $Apc^{Min/+}$·*AhR*-disrupted mice, suggesting that AhR-mediated β-catenin degradation has a suppressive role in intestinal carcinogenesis in parallel to the Apc system.

Tumor Suppression by AhR Natural Ligands. As described in Fig. 3, IAA and I3C accelerated β-catenin degradation in the intestine.

We were interested to study whether natural AhR ligands actually suppress carcinogenesis in the cecum or small intestine in $Apc^{Min/+}$ mice (Fig. 5). The chemoprevention (30) study was designed so that $Apc^{Min/+}$ or $Apc^{Min/+}$·$AhR^{+/-}$ mice were fed natural AhR ligand-containing diets, such as I3C (31) and DIM (32), immediately after weaning at 3–4 weeks of age. When fed the control diet, $Apc^{Min/+}$ mice started to develop small intestinal polyps at 7 weeks of age with the number of tumors containing polyps plateauing (≈30 tumors per mouse) at ≈10 to 15 weeks (Fig. 5*B*), whereas the cecal tumor incidence was as described (Figs. 4*A* and 5*A*). However, when fed an I3C (0.1%)- or DIM (0.01%)-containing diet, $Apc^{Min/+}$ mice showed a cecal tumor incidence of ≈50% of the total at 25 weeks of age (Fig. 5*A*) and a markedly reduced number of tumors in the small intestine (Fig. 5*B*). Similar chemopreventive effects were also clearly observed with the compound $Apc^{Min/+}$·$AhR^{+/-}$ mutant mice (Fig. 5*C* and *D*). However, no suppressive effect was observed in $AhR^{-/-}$ mice (Fig. S7*D*), suggesting that AhR ligand-dependent chemoprevention requires the presence of AhR.

Using immunohistochemical analysis, we showed a marked reduction of β-catenin except for the molecules associated with adherence junctions in the intestines of $Apc^{Min/+}$ (Fig. 5*E*; Fig. S7*F*) and $Apc^{Min/+}$·$AhR^{+/-}$ mice (Fig. S7 *E* and *F*) fed AhR ligand-containing diets compared with those fed a control diet. These results clearly demonstrate that chemoprevention of intestinal carcinogenesis by AhR ligands in $Apc^{Min/+}$ and $Apc^{Min/+}$·$AhR^{+/-}$ mice is due to β-catenin degradation mediated by the natural ligand-activated AhR E3 ubiquitin ligase.

Discussion

In this study, we provide both loss-of-function and gain-of-function data to show that the AhR mediates ligand-dependent degradation of β-catenin, leading to suppression of intestinal carcinogenesis. The AhR-mediated pathway of β-catenin degradation is independent of the canonical APC-mediated pathway, but functions cooperatively with it, because (*i*) $AhR^{-/-}$ mice develop colonic tumors mostly in the cecum, whereas numerous polyps develop mostly in the small intestine of $Apc^{Min/+}$ mice; (*ii*) even in cells containing mutations in APC or β-catenin gene, β-catenin is clearly degraded in an AhR ligand-dependent manner; and (*iii*) experiments using siRNAs against AhR, its E3 ubiquitin ligase cofactor CUL4B, and APC clearly indicate the independency between the 2 pathways. The cooperative function is strongly confirmed by additional experiments, in which (*i*) accelerated carcinogenesis was observed in the compound $Apc^{Min/+}$·*AhR*-disrupted mutant mice compared with $Apc^{Min/+}$ mice, and (*ii*) AhR natural ligands suppress intestinal carcinogenesis in $Apc^{Min/+}$ mice. These distinct roles are most likely because the AhR- and APC-dependent β-catenin degradation pathways are considered to be in different subcellular compartments (Fig. S8*A*); ligand-activated AhR translocates to the nucleus where it forms an ubiquitylation complex containing CUL4B (7) and the constitutively nuclear protein Arnt, whereas the APC-dependent pathway functions in the cytoplasm (33–35).

It is noteworthy that $AhR^{-/-}$ mice mainly develop tumors in the cecum, but not in the small intestine, whereas numerous polyps develop mostly in the small intestine of $Apc^{Min/+}$ mutant mice (29). Our findings that AhR is abundantly expressed in Paneth cells of the small intestine, as well as the cecum near the ileocecal junction, and that abnormal β-catenin accumulation is observed in the intestines of $AhR^{-/-}$ mice, suggest that intestines of $AhR^{-/-}$ mice may be in a cancer-prone or precancerous state (23). Although it is still unknown why $AhR^{-/-}$ mice specifically develop cecal cancers, the host genetic predisposition to these cancers may be potentiated by stimuli from bacteria colonized in the cecum (36). Abnormal β-catenin accumulation, together with microbial interaction or subsequent inflammation, may promote cecal carcinogenesis in $AhR^{-/-}$ mice. In conjunction with the involvement of intestinal microbes, different structural and functional properties of intestinal epithelial cells (34) may also be associated with the specific development of cecal tumor in $AhR^{-/-}$ mice.

We show evidence that natural AhR ligands converted from dietary Trp and glucosinolates in the intestine are as efficient as exogenous AhR ligands in promoting degradation of endogenous β-catenin. These results provide a molecular basis for chemopreventive mechanisms against intestinal carcinogenesis that were observed in $Apc^{Min/+}$ and $Apc^{Min/+}$·$AhR^{+/-}$ mice fed diets containing the AhR ligands I3C and DIM. Also, our findings lend credence to previous reports on the chemopreventive effects on colorectal cancers in humans by cruciferous vegetables that contain a high content of glucosinolates (16–18), and suggest that AhR ligands define a potent strategy for dietary chemoprevention of intestinal cancer.

In conclusion, this study shows that AhR has a critical role in suppression of intestinal carcinogenesis by a previously undescribed ligand-dependent mechanism of proteasomal degradation of β-catenin, which functions independently of and cooperatively with the canonical APC-dependent pathway. $AhR^{-/-}$ mice provide a murine model for spontaneously developing tubular adenocarcinomas, which have the most common histologic characteristics of sporadic colorectal cancers in humans. Although the reasons remain to be established, reduced AhR expression was observed in 12 specimen of human cecal cancers and their surrounding tissues (Fig. S4). Together, we conclude that $AhR^{-/-}$ mice are a useful model to study human intestinal cancer, and will help us to investigate the molecular mechanisms of pathogenesis and chemoprevention of intestinal cancer.

Materials and Methods

Animal Experiments. C57BL/6 wild-type and *AhR*-deficient ($AhR^{-/-}$) (4) mice on the C57BL/6 background were obtained from CLEA Japan. $Apc^{Min/+}$ mice (29) on a C57BL/6 genetic background were purchased from The Jackson Laboratory. Generation of germ-free (GF) mice or compound $Apc^{Min/+}$·*AhR*-disrupted mutant mice, carcinogenesis, and chemoprevention studies were performed as described in the *SI Materials and Methods*. All animal experiments were approved by the Saitama Cancer Center Animal Care and Use Committee.

Biochemical Analyses. Immunohistochemistry was performed on 4–5 μm sequential paraffin sections using the antibodies described. Total RNA was extracted from the intestines of $AhR^{+/+}$ or $AhR^{-/-}$ mice using an Isogen kit (Nippon Gene), and RT-PCR was performed using TaKaRa RNA PCR kits (Takara Shuzo). Cell culture and transfection assays were performed using standard methods. Protein stability analysis and in vitro ubiquitylation assay were performed as previously reported (6). Sequences of the siRNAs used in this study and HPLC analysis are described in *SI Materials and Methods*.

Statistical Analyses. Differences in survival in the mouse genotypes were analyzed using the Kaplan-Meyer method, and statistical analyses were performed with the log-rank test. We analyzed numeric data for statistical significance using the Student's *t* test. We considered $P < 0.05$ as significant.

ACKNOWLEDGMENTS. We thank Drs. T. Omura and M. Suganuma for valuable comments, and Ms. S. Nakabayashi for technical assistance. This work was supported in part by the Solution Oriented Research for Science and Technology Agency (K.K. and Y.F.-K), by grants-in-aid from the Ministry of Education, Culture, Sports, Science, and Technology of Japan (K.K), and by a grant for Scientific Research from the Ministry of Health, Labor, and Welfare of Japan (to Y.F.-K).

1. Gu YZ, Hogenesch J, Bradfield CA (2000) The PAS superfamily: Sensors of environmental and developmental signals. *Annu Rev Pharmacol* 40:519–561.
2. Fujii-Kuriyama Y, Mimura J (2005) Molecular mechanisms of AhR functions in the regulation of cytochrome *P450* genes. *Biochem Biophys Res Commun* 338:311–317.
3. Nebert DW, Dalton TP (2006) The role of cytochrome P450 enzymes in endogenous signalling pathways and environmental carcinogenesis. *Nat Rev Cancer* 6:947–960.
4. Mimura J, et al. (1997) Loss of teratogenic response to 2,3,7,8-tetrachlorodibenzo-*p*-dioxin (TCDD) in mice lacking the Ah (dioxin) receptor. *Genes Cells* 2:645–654.

5. Shimizu Y, et al. (2000) Benzopyrene carcinogenicity is lost in mice lacking the aryl hydrocarbon receptor. *Proc Natl Acad Sci USA* 97:779–782.
6. Ohtake F, et al. (2007) Dioxin receptor is a ligand-dependent E3 ubiquitin ligase. *Nature* 446:562–566.
7. Quintana FJ, et al. (2008) Control of T_{reg} and T_H17 cell differentiation by the aryl hydrocarbon receptor. *Nature* 453:65–71.
8. Veldhoen M, et al. (2008) The aryl hydrocarbon receptor links T_H17-cell-mediated autoimmunity to environmental toxins. *Nature* 453:106–109.
9. Kimura A, Naka T, Nohara K, Fujii-Kuriyama Y, Kishimoto T (2008) Aryl hydrocarbon receptor regulates Stat1 activation and participates in the development of Th17 cells. *Proc Natl Acad Sci USA* 105:9721–9726.
10. Ikuta T, Kobayashi Y, Kawajiri K (2004) Cell density regulates intracellular localization of aryl hydrocarbon receptor. *J Biol Chem* 279:19209–19216.
11. Lee S, et al. (1996) Nuclear/cytoplasmic localization of the von Hippel-Lindau tumor suppressor gene product is determined by cell density. *Proc Natl Acad Sci USA* 93:1770–1775.
12. Zhang F, White RL, Neufeld KL (2001) Cell density and phosphorylation control the subcellular localization of adenomatous polyposis coli protein. *Mol Cell Biol* 21:8143–8156.
13. Nguyen LP, Bradfield CA (2008) The search for endogenous activators of the aryl hydrocarbon receptor. *Chem Res Toxicol* 21:102–116.
14. Heath-Pagliuso S, et al. (1998) Activation of the Ah receptor by tryptophan and tryptophan metabolites. *Biochemistry* 37:11508–11515.
15. Bjeldanes LF, et al. (1991) Aromatic hydrocarbon responsiveness-receptor agonists generated from indole-3-carbinol *in vitro* and *in vivo*: Comparisons with 2,3,7,8-tetrachlorodibenzo-*p*-dioxin. *Proc Natl Acad Sci USA* 88:9543–9547.
16. Kim YS, Milner JA (2005) Targets for indole-3-carbinol in cancer prevention. *J Nut Biochem* 16:65–73.
17. Bonnesen C, Eggleston IM, Hayes JD (2001) Dietary indoles and isothiocyanates that are generated from cruciferous vegetables can both stimulate apoptosis and confer protection against DNA damage in human colon cell lines. *Cancer Res* 61:6120–6130.
18. Potter JD, Steinmetz K (1996) Vegetables, fruit, and phytoestrogens as preventive agents. *IARC Sci Publ* 139:61–90.
19. Fernandez-Salguero PM, Ward JM, Sundberg JP, Gonzalez FJ (1997) Lesions of aryl hydrocarbon receptor-deficient mice. *Vet Pathol* 34:605–614.
20. McMillan BJ, Bradfield CA (2007) The aryl hydrocarbon receptor sans xenobiotics: Endogenous function in genetic model system. *Mol Pharmacol* 72:487–498.
21. He TC, et al. (1998) Identification of c-*MYC* as a target of the APC pathway. *Science* 281:1509–1512.
22. van Es JH, et al. (2005) Wnt signalling induces maturation of Paneth cells in intestinal crypts. *Nat Cell Biol* 7:381–386.
23. van de Wetering M, et al. (2002) The β-catenin/TCF-4 complex imposes a crypt progenitor phenotype on colorectal cancer cells. *Cell* 111:241–250.
24. Yang J, et al. (1997) Adenomatous polyposis coli (APC) differentially regulates β-catenin phosphorylation and ubiquitination in colon cancer cells. *J Biol Chem* 281:17751–17757.
25. Liu C, et al. (1999) β-Trcp couples β-catenin phosphorylation-degradation and regulates *Xenopus* axis formation. *Proc Natl Acad Sci USA* 96:6273–6278.
26. Kinzler KW, et al. (1991) Identification of FAP locus genes from chromosome 5q21. *Science* 253:661–665.
27. Nishisho I, et al. (1991) Mutations of chromosome 5q21 genes in FAP and colorectal cancer patients. *Science* 253:665–669.
28. Kinzler KW, Vogelstein B (1996) Lessons from hereditary colorectal cancer. *Cell* 87:159–170.
29. Moser AR, Pitot HC, Dove WF (1990) A dominant mutation that predisposes to multiple intestinal neoplasia in the mouse. *Science* 247:322–324.
30. Wattenberg LW (1985) Chemoprevention of cancer. *Cancer Res* 45:1–8.
31. Xu M, et al. (1996) Protection by green tea, black tea, and indole-3-carbinol against 2-amino-3-methylimidazo[4,5-*f*]quinoline-induced DNA adducts and colonic aberrant crypts in the F344 rat. *Carcinogenesis* 17:1429–1434.
32. Chen I, McDougal A, Wang F, Safe S (1998) Aryl hydrocarbon receptor-mediated antiestrogenic and antitumorigenic activity of diindolylmethane. *Carcinogenesis* 19:1631–1639.
33. Fearon ER, Vogelstein B (1990) A genetic model for colorectal tumorigenesis. *Cell* 61:759–767.
34. Reya T, Clevers H (2005) Wnt signaling in stem cells and cancer. *Nature* 434:843–850.
35. Kitagawa M, et al. (1999) An F-box protein, FWD1, mediates ubiquitin-dependent proteolysis of β-catenin. *EMBO J* 18:2401–2410.
36. Maggio-Price L, et al. (2006) *Helicobacter* infection is required for inflammation and colon cancer in Smad3-deficient mice. *Cancer Res* 66:828–838.

Arch Toxicol (2009) 83:795–803
DOI 10.1007/s00204-009-0420-4

MOLECULAR TOXICOLOGY

Benzene activates caspase-4 and -12 at the transcription level, without an association with apoptosis, in mouse bone marrow cells lacking the p53 gene

Jung-Yeon Yi · Yoko Hirabayashi · Yang-Kyu Choi · Yukio Kodama · Jun Kanno · Jeong-Hee Han · Tohru Inoue · Byung-Il Yoon

Received: 11 November 2008 / Accepted: 10 March 2009 / Published online: 27 March 2009

Abstract Benzene is a well-known environmental pollutant that can induce hematotoxicity, aplastic anemia, acute myelogenous leukemia, and lymphoma. However, although benzene metabolites are known to induce oxidative stress and disrupt the cell cycle, the mechanism underlying lympho/leukemogenicity is not fully understood. Caspase-4 (alias caspase-11) and -12 are inflammatory caspases implicated in inflammation and endoplasmic reticulum stress-induced apoptosis. The objectives of this study were to investigate the altered expression of caspase-4 and -12 in mouse bone marrow after benzene exposure and to determine whether their alterations are associated with benzene-induced bone marrow toxicity, especially cellular apoptosis. In addition, we evaluated whether the p53 gene is involved in regulating the mechanism, using both wild-type (WT) mice and mice lacking the p53 gene. For this study, 8-week-old C57BL/6 mice [WT and p53 knockout (KO)] were administered a benzene solution (150 mg/kg diluted in corn oil) via oral gavage once daily, 5 days/week, for 1 or 2 weeks. Blood and bone marrow cells were collected and cell counts were measured using a Coulter counter. Total mRNA and protein extracts were prepared from the harvested bone marrow cells. Then qRT-PCR and Western blotting were performed to detect changes in the caspases at the mRNA and protein level, respectively. A DNA fragmentation assay and Annexin-V staining were carried out on the bone marrow cells to detect apoptosis. Results indicated that when compared to the control, leukocyte number and bone marrow cellularity decreased significantly in WT mice. The expression of caspase-4 and -12 mRNA increased significantly after 12 days of benzene treatment in the bone marrow cells of benzene-exposed p53KO mice. However, apoptosis detection assays indicated no evidence of apoptosis in p53KO or WT mice. In addition, no changes of other apoptosis-related caspases, such as caspase-3 and -9, were found in WT or p53KO mice at the level of mRNA and proteins. These results indicated that upregulation of caspase-4 and -12 in mice lacking the p53 gene is not associated with cellular apoptosis. In conclusion, caspase-4 and -12 can be activated by benzene treatment without inducing cell apoptosis in mouse bone marrow, which are partly under the regulation of the p53 gene.

Keywords Apoptosis · Benzene · Bone marrow · Caspase-4 · Caspase-12 · Mouse, p53

J.-Y. Yi and Y. Hirabayashi contributed equally for this study.

J.-Y. Yi · J.-H. Han · B.-I. Yoon (✉)
School of Veterinary Medicine, Kangwon National University,
192-1 Hyoja 2, Chuncheon, Gangwon 200-701, Republic of Korea
e-mail: byoon@kangwon.ac.kr

Y. Hirabayashi · Y. Kodama · J. Kanno
Division of Cellular and Molecular Toxicology,
Center for Biological Safety and Research,
National Institute of Health Sciences, Tokyo, Japan

Y.-K. Choi
College of Veterinary Medicine, Konkuk University,
Seoul, Republic of Korea

T. Inoue
Biological Safety and Research Center,
National Institute of Health Sciences, Tokyo, Japan

Introduction

Benzene is a well-known environmental pollutant found in gasoline, automobile exhaust, and cigarette smoke (Lynge et al. 1997; Rana and Verma 2005; Wallace 1996). Exposure to benzene is associated with hematotoxicity, which

may give rise to aplastic anemia, acute myelogenous leukemia, and lymphoma (Brief et al. 1980; Cronkite 1986; Farris et al. 1997; Huff et al. 1989; Rinsky et al. 1981; Snyder et al. 1980; Snyder et al. 1988). Furthermore, benzene has been postulated to have multisite carcinogenicity because it leads to tumor development in various organs such as lung, oral cavity, Harderian gland, mammary gland, and skin (Huff et al. 1989; Maltoni et al. 1989; Snyder et al. 1988). Once absorbed, benzene is metabolized into a variety of intermediate compounds, including benzene oxide, phenol, catechol, hydroquinone, and benzoquinone. This conversion occurs in several organs, including the liver and bone marrow (Snyder and Hedli 1996). Phenol metabolites derived from benzene oxide via cytochrome P450 2E1 (CYP2E1) (Ross 2000) are believed to generate reactive oxygen species (ROS) after hydroxylation by myeloperoxidase. Once the oxidative aggression surpasses the antioxidant defense system in cells, the resultant oxidative stress can induce hematolymphoid toxicity in bone marrow (Hiraku and Kawanishi 1996; Kuo et al. 1999). However, the mechanism underlying lympho/leukemogenicity is not fully understood, although benzene metabolites are known to induce oxidative stress and disrupt the cell cycle (Danial and Korsmeyer 2004; Rao and Snyder 1995; Yoon et al. 2001).

Caspase-4 and -12 are inflammatory caspases, characterized by the presence of a large prodomain containing a typical caspase recruitment domain (CARD) at the N-terminus (Martinon and Tschopp 2007). Caspase-4 is proinflammatory in that it activates caspase-1, while caspase-12 is considered to function as a negative regulator of the inflammatory signaling pathway (Lamkanfi et al. 2007). However, their precise functions and regulatory mechanisms remain elusive. In addition to the implications of the caspases in inflammation, they are also thought to be involved in apoptosis of specific cell populations, such as nerve cells (Fan et al. 2005; Hisahara et al. 2001; Kang et al. 2000; Scott and Saleh 2007; Suk et al. 2002). According to previous studies, activation of caspase-4 and -12 is mediated via both p53-dependent and -independent pathways, depending on the pathogenic situation (Choi et al. 2001; Fábián et al. 2007), but their alterations and possible roles have not been studied in association with the underlying mechanisms of benzene toxicity. Recently, microarray analyses indicated that caspase-4 can be activated in benzene-exposed mouse bone marrow (Yoon et al. 2003), suggesting that they could play some roles in the action mechanisms of benzene in the bone marrow, via either p53-mediated or independent mechanisms.

Thus, in the present study, we investigated the altered expression of caspase-4 and -12 in the mouse bone marrow following benzene exposure and explored whether their alterations are associated with benzene-induced bone marrow toxicity, especially cellular apoptosis. Furthermore, we evaluated whether the p53 gene is implicated in regulating the mechanism using both wild-type (WT) mice and mice lacking the p53 gene.

Materials and methods

Animals

The targeting vector for the *Trp*53 gene, a 2.8-kb recombinant plasmid containing a neomycin-resistant gene just before the transcriptional starting site, was inserted into TT2 embryonic stem cells (heterozygous for C57BL/6 and CBA; Yagi et al. 1993) to establish the homologous recombinant clones (Tsukada et al. 1993). By means of an aggregation chimera with the recombinant clones, chimeric mice were produced, followed by establishing *Trp*53-knockout mice in 1987 after confirmation of the germinal transmission of *Trp*53-deficient (C57BL/6 × CBA) F1 mice (Tsukada et al. 1993). General information about the recombinant mice is also available elsewhere (*Trp*53^{tm1Sia} MGI: 1926340, Mouse Genome Informatics 2009). The original *Trp*53-deficient (C57BL/6 × CBA) F1 mice crossed back into C57BL/6 were transferred to the animal facility of the National Institute of Health Sciences (NIHS, Tokyo, Japan) at the second generation. Backcrossing into C57BL/6 occurred over 20 generations in 1997 and their backcrossing has been continuously maintained.

In this study, male WT and homozygous *Trp*53-deficient mice were used. The homozygous *Trp*53-deficient mice and WT mice were generated by mating between heterozygous *Trp*53-deficient mice at the animal facility of the NIHS. Neonates were genotyped by primer for the targeted DNA sequence, including a partial *neo* gene on the 5′ side of exon 4 by polymerase chain reaction (PCR) analysis using tissue obtained from the tail (Hirabayashi et al. 2002; Tsukada et al. 1993; Yoshida et al. 2002). Genotyping was conducted using five 8-week-old mice for each genotype. During the study, the mice were kept on a 12-h light–dark cycle, an autoclave-sterilized basal pellet diet (CRF-1: Oriental Yeast Co., Ltd., Tokyo, Japan) and distilled water were provided ad libitum throughout the study. Temperature and humidity were maintained automatically at 24 ± 1°C and 55 ± 10%, respectively.

All animals were maintained in the board-approved laboratory animal facility of the NIHS. All experimental protocols involving the laboratory mice used in this study were reviewed by the Interdisciplinary Monitoring Committee for the Proper Animal Use and Welfare of Experimental Animals (ICRAW), a peer reviewed panel established at the NIHS, and approved by the Committee for Animal Care and Use (CACU) of the NIHS and the Institutional Animal

Care and Use Committee (IACUC) at Kangwon National University for compliance with the National Research Council's Guide for the Care and Use of Laboratory Animals (NRC 1996). All animal studies were conducted using humane protocols approved by the CACU and Kangwon National University.

Benzene exposure

Benzene (CAS No. 319953; Sigma-Aldrich, St. Louis, MO, USA) was diluted in corn oil (CAS No. C8267; Sigma-Aldrich) and administered via oral gavage in a single dose of 150 mg/kg in a volume of 10 ml/kg b.w. once daily, 5 days/week, for 1 or 2 weeks; this protocol was shown to create an effect on mouse bone marrow similar in grade to the effect produced when 300 ppm benzene is inhaled (Yi and Yoon 2008). The sham control groups were administrated corn oil (Sigma-Aldrich) alone during the same period. The mice were killed 2 h after the last treatment; and peripheral blood and bone marrow cells were then harvested. The experimental schedules for sham and benzene-treated mice are shown in Fig. 1. Five mice per group were used for each experiment.

Peripheral blood and bone marrow harvesting

Blood and bone marrow cells were collected from the orbital sinus and both femora of each mouse, respectively; then peripheral blood and bone marrow cell counts were performed using a blood cell counter (Sysmex K-4500; Sysmex, Tokyo, Japan).

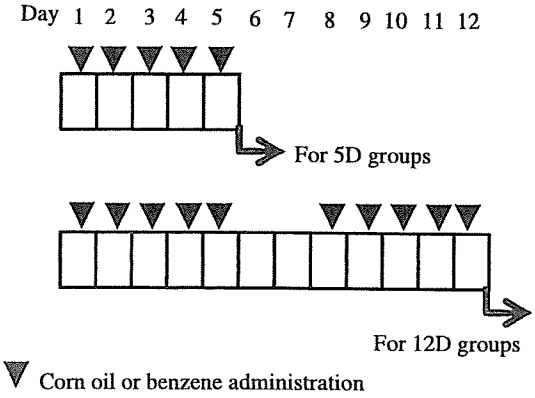

Fig. 1 Experimental protocol. Benzene (150 mg/kg) or vehicle alone (corn oil) was administered by oral gavage once daily, 5 days/week, for 1 or 2 weeks. The mice were killed 4 h after the final treatment on day 5 or day 12 and bone marrow cells were harvested from both femora of each individual

Collection of bone marrow cells

Bone marrow cells were harvested from both femora of each mouse. Bone marrow cells were flushed out of the bone shaft using a 27-gauge hypodermic needle filled with 2 ml of Dulbecco's modified minimum Eagle's medium (DMEM) without phenol red (Invitrogen, Carlsbad, CA, USA). The bone marrow cells were then passed repeatedly through a needle to produce a single-cell suspension. After lysis of red blood cells, a portion of the bone marrow cells was subjected to total RNA extraction using TRIzol reagent (Invitrogen), and the remaining cells were frozen in liquid nitrogen and stored at −80°C until required for Western blotting or DNA fragmentation analysis.

PCR for genotyping

To detect *Trp*53 WT and *Trp*53-deficient alleles, PCR was performed using genomic DNA extracted from the tail of each mouse, and synthetic oligonucleotides were used as primers as described elsewhere (Tsukada et al. 1993). Briefly to detect the *Trp*53 WT allele, the 5′ common primer (5′-aattgacaagttatgcatcca-3′) and the 3′ primer (5′-actcctcaacatcctggggcagcaacagat-3) were used; to detect the *Trp*53-deficient allele, the 5′ common primer and *neo sequence* primer (5′-gaacctgcgtgcaatccatcttgttcaatg-3′) were used.

Annexin-V staining

Bone marrow cells harvested from vehicle- and benzene-treated mice were suspended in an annexin-V-fluorescein isothiocyanate (FITC) binding buffer at a final concentration of 1×10^6 cells/ml. Annexin-V staining was performed according to the manufacturer's protocol and quantified using a flow cytometer (Beckman-Coulter, Miami, FL, USA).

DNA fragmentation assay

To detect DNA fragmentation in bone marrow cells, DNA laddering assays were performed using a commercially available kit (Roche, Mannheim, Germany) according to the manufacturer's protocol. Briefly, the harvested bone marrow cells were mixed with 180 µl of phosphate-buffered saline (PBS) and 200 µl of binding/lysis buffer. The suspensions were incubated for 10 min at room temperature and then shaken after adding 100 µl of isopropanol. The samples were pipetted into the upper reservoir of a combined filter and collection tube, and then centrifuged for 1 min at 8,000 rpm. After discarding the flow-through solution, 500 µl of washing buffer was added to the upper reservoir and the tube was centrifuged again for 1 min at 8,000 rpm.